National Defence Défense nationale

DEFENCE RESEARCH AND DEVELOPMENT CANADA (DRDC)
RECHERCHE ET DÉVELOPPEMENT POUR LA DÉFENSE CANADA (RDDC)

Soundscape Characterization and Marine Mammal Occurrence

Western Baffin Bay, September 2022–23

Julien Delarue
Colleen Wilson
Allison Richardson
JASCO Applied Sciences

Prepared by:
JASCO Applied Sciences (Canada) Ltd
20 Mount Hope Avenue
Dartmouth, NS B2Y 4S3

Contractor Document Number: R.127481.001, PO 700748104
Technical Authority: Sean Pecknold, Defence Scientist
Contractor's Date of Publication: March 2024

Defence Research and Development Canada

Contract Report
DRDC-RDDC-2024-C167
July 2024

Canada

IMPORTANT INFORMATIVE STATEMENTS

This document was reviewed for Controlled Goods by Defence Research and Development Canada using the Schedule to the *Defence Production Act*.

Soundscape Characterization and Marine Mammal Occurrence

Western Baffin Bay, September 2022–23

JASCO Applied Sciences (Canada) Ltd

26 March 2024

Submitted to:

Sean Pecknold
Defense Research & Development Canada (DRDC)
PO 700748104

Authors:

Julien J.-Y. Delarue
Colleen C. Wilson
Allison Richardson

P001689-002
Document 03340
Version 1.0

JASCO APPLIED SCIENCES

Suggested citation:

Delarue, J.J.-Y., C.C. Wilson, and A. Richardson. 2024. Soundscape Characterization and Marine Mammal Occurrence: Western Baffin Bay, September 2022–23. Document 03340, Version 1.0. Technical report by JASCO Applied Sciences for Defense Research & Development Canada (DRDC).

Report approved by:

Version	*Role*	*Name*	*Date*
1.0	Project Manager Senior Scientific Reviewer	Bruce Martin	12 Mar 2024

Disclaimer: The results presented herein are relevant within the specific context described in this report. They could be misinterpreted if not considered in the light of all the information contained in this report. Accordingly, if information from this report is used in documents released to the public or to regulatory bodies, such documents must clearly cite the original report, which shall be made readily available to the recipients in integral and unedited form.

Authorship statement: Individual authors of this report may have only contributed to portions of the document and thus not be responsible for the entire content. This report may contain standardized (boilerplate) components that are common property of JASCO and are not directly attributed to their original authors/creators. The entire content of this report has been subject to senior scientific review by the qualified person listed in the front matter of the document.

Contents

Figures

Tables

1. Introduction

JASCO Applied Sciences (JASCO) was contracted by Defense Research & Development Canada (DRDC) to assist with the analysis of long-term Passive Acoustic Monitoring (PAM) data from Baffin Bay. DRDC deployed three moorings with Autonomous Multi-channel Acoustic Recorders (AMARs) along the western side of Baffin Bay in August of 2022 and retrieved them in September 2023 (Figure 1). JASCO was tasked with downloading the three year-long AMAR recordings and performing a basic analysis of the data to identify data quality issues, if any, and to characterize ambient sound and provide a basic description of vessel and marine mammal presence. This report presents the results of these analyses and identifies topics worthy of further investigation.

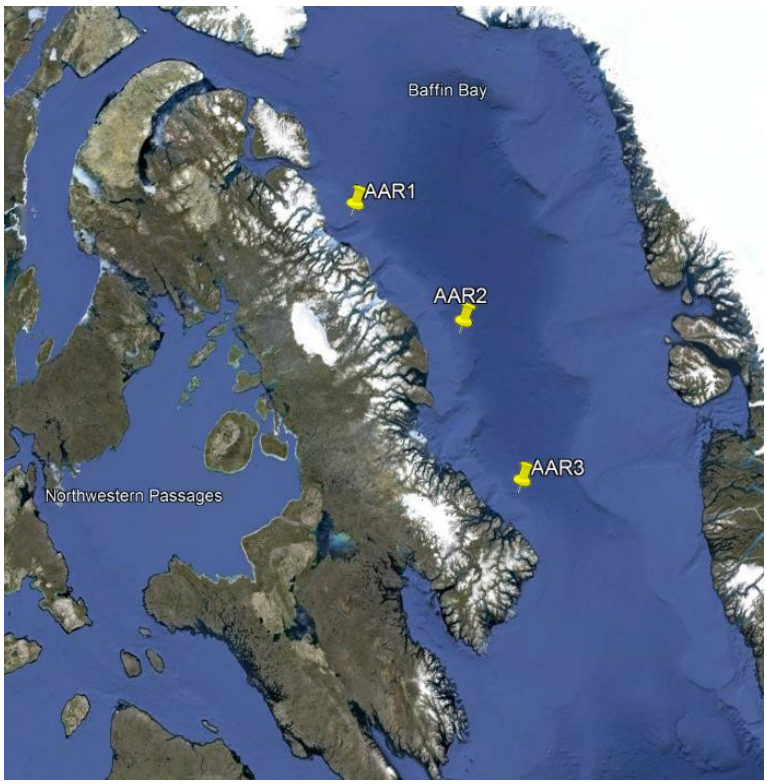

Figure 1. Location of the three acoustic recorders deployed between August 2022 and September 2023 in this study.

1.1. Ambient Ocean Soundscape

The acoustic environment of a location is known as its soundscape. A soundscape is comprised of the cumulative contributions from abiotic (geophonic), biotic (biophonic), and human (anthrophonic) sound sources (Krause 2008). Ambient sound is defined as any sound present in the absence of human activity. It is also temporally and spatially specific (ISO 2017a). The Wenz (1962) curves in Figure 2 show the typical frequencies and spectral levels of many of these activities.

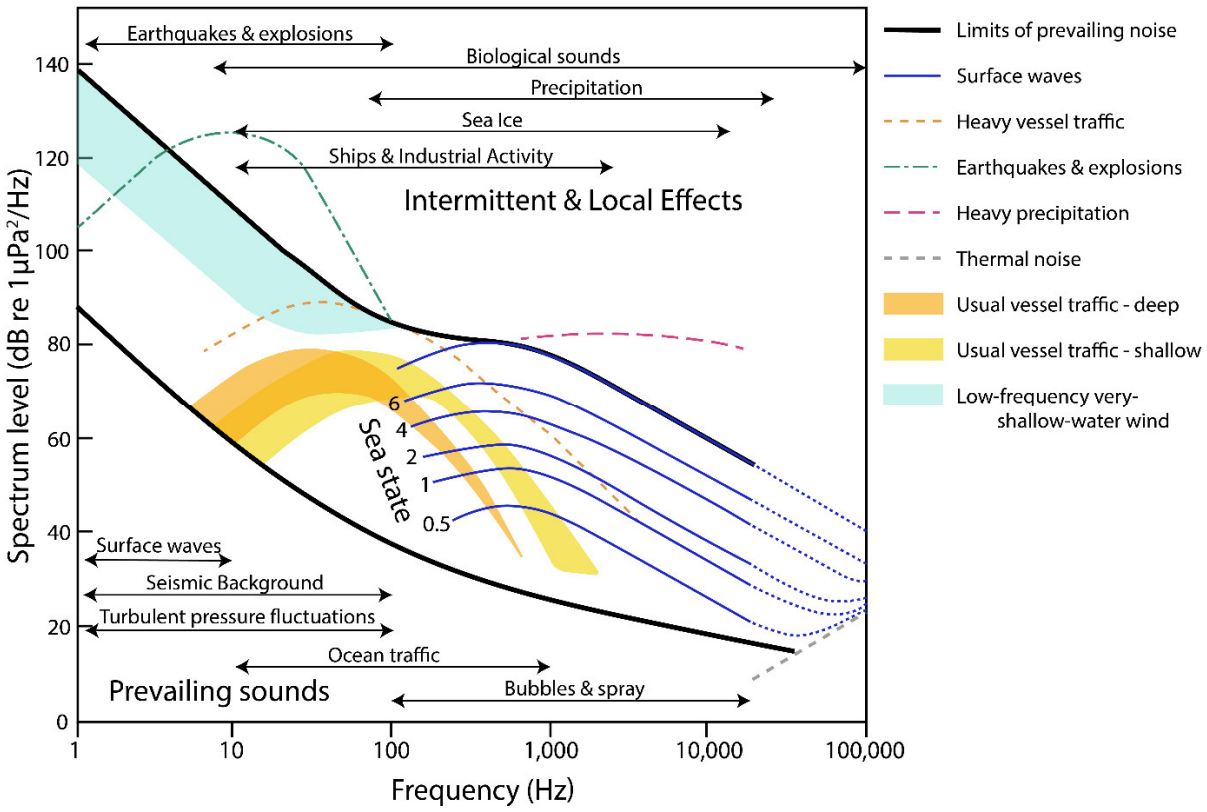

Figure 2. Wenz curves describing pressure spectral density levels of marine ambient sound from weather, wind, geologic activity, and commercial shipping (adapted from NRC 2003, based on Wenz 1962). The thick lines are the limits of prevailing ambient sound, which are included in some of the results plots to provide context.

In the marine environment, the geophonic elements of a soundscape can act as proxies for oceanographic conditions. Knudsen et al. (1948) and Wenz (1962) demonstrated that increased sea state and wind speed commonly correlate with higher sound intensities across frequencies from 500 Hz to 30 kHz due to breaking whitecaps, surface flow noise, wave generation, cavitation, and pressure change (Urick 1983). Rainfall can elevate sound levels in the 1–15 kHz frequency range via sound from surface impacts and bubble entrainment (Heindsmann et al. 1955, Bom 1969, Scrimger et al. 1987).

In high latitude areas, ice can be a prominent feature of a soundscape. The contribution of sea ice is usually highest when it is forming and breaking up. Under established sea ice, sound levels are usually lower than in open water areas because the ice attenuates or even eliminates the effects of wind and waves on the soundscape (Menze et al. 2017). Waves, sea ice, currents, and seismic activity (such as earth movement and subsea landslides) can also be loud, though short-duration, geophonic contributors.

While geophonic and biophonic contributors comprise the natural soundscape, the total soundscape also includes anthrophonic (related to human activity) sounds.

Human sound sources are diverse and can have large underwater acoustic footprints. The main sources are vessel noise, which is primarily caused by global shipping vessels, and seismic exploration for hydrocarbon deposits. The development of offshore wind farms and other coastal construction projects are also important sound sources, although more restricted in their impact areas. Military activities (e.g., sonar use) can also have also substantial footprint and negative impacts on marine life but are generally rare and short-duration events.

Measuring ambient sound and characterizing the soundscape of an area is complicated by non-acoustic processes that often appear in acoustic recordings. One such issue is flow noise, which is caused by pressure eddies and vortices produced by water moving along the surfaces of hydrophone pressure transducers. This is similar to the buffeting sounds recorded by microphones in the wind. Flow noise is not part of a marine soundscape (Strasberg 1979, Urick 1983), but its intensity may indicate current strength (Willis and Dietz 1961). Current or wave action can also induce mooring noise when non-stationary components of a mooring create sound as they move or strum.

1.2. Anthropogenic Contributors to the Soundscape

Anthropogenic (human-generated) sound can be a by-product of vessel operations, such as engine sound radiating through vessel hulls and cavitating propulsion systems, or it can be a product of active acoustic data collection with seismic surveys, military sonar, hull-cleaning acoustic devices and depth sounding as the main contributors. Marine construction projects often involve nearshore blasting and pile driving that can produce high levels of impulsive-type noise. The contribution of anthropogenic sources to the ocean soundscape has increased from the 1950s to 2010, largely driven by greater maritime shipping traffic (Ross 1976, Andrew et al. 2011). Recent trends suggest that global sound levels are leveling off or potentially decreasing in some areas (Andrew et al. 2011, Miksis-Olds and Nichols 2016). Oil and gas exploration with seismic airguns, marine pile driving, and oil and gas production platforms elevate sound levels over radii of 10 to 1000 km when present (Bailey et al. 2010, Miksis-Olds and Nichols 2016, Delarue et al. 2018). The extent of seismic survey sounds has increased substantially following the expansion of oil and gas exploration into deep water, and seismic sounds can now be detected across ocean basins (Nieukirk et al. 2004).

The main anthropogenic contributor to ambient sound in the present study was vessel noise associated with fishing activities, primarily distributed along the continental slope, and limited vessel traffic. As expected due to the remote location of the study area, in deep waters off the eastern side of Baffin Island, anthropogenic activities are much reduced compared to areas further south closer to population centers and global shipping lanes. In addition, sea ice covers prevents access to the area for most vessels between November and June.

1.3. Soniferous Marine Life and Acoustic Monitoring

The long-term monitoring of marine species in remote areas is challenging but is important for understanding the temporal and spatial distributions of animals and for designing conservation measures for species at risk. Visual monitoring techniques are important, but can be limited spatially, temporally, and rely on good visibility conditions. Given that most marine mammals produce sounds underwater, acoustic monitoring is generally an effective way to monitor for the presence of multiple species of marine mammals in remote environments year-round. Compared to visual techniques, acoustic monitoring depends less on weather conditions and is unaffected by visibility. However, acoustic monitoring requires animals to make sounds and those sounds must be sufficiently loud to be detected. Because not all species vocalize regularly, and vocalization activity often depends on season, acoustic monitoring effectiveness varies by species and seasonally.

For an acoustic recording device to detect a vocalization, its received amplitude at the monitoring location must be above background noise levels in at least one of the vocalization's frequency bands (although some more complex acoustic systems can detect sounds below background noise level). The distance over which vocalizations can be detected consequently depends on the background sound levels, source levels of the vocalization (which often vary by season, sex, etc.), calling depth of the animal, and acoustic propagation properties of the environment. Background or ambient sound levels vary due to fluctuations in natural sounds (e.g., wind, precipitation, waves, seismic activity, and biologic activity) and anthropogenic sounds (mainly vessels but also marine construction and oil and gas exploration). Acoustic propagation also varies seasonally due to changing temperature and salinity properties of the water column.

Passive acoustic monitoring relies on the monitored species to produce detectable sound. Several marine taxa produce sounds. For non-mammal species, although crustaceans and other aquatic invertebrates have been documented as capable of producing sound, the practical use of acoustic monitoring to date has largely been limited to fish. Many fish species produce sound during the breeding season or when engaged in agonistic behaviours (Amorim 2006). Several species of gadids (cod family), such as Northern cod (*Gadus morhua*) and haddock (*Melanogrammus aeglefinus*), form spawning aggregations that have been detected acoustically (Nordeide and Kjellsby 1999, Hawkins et al. 2002). The acoustic monitoring of fish is hindered by a limited understanding of their acoustic repertoire and behaviour. Nevertheless, the stereotypical nature of acoustic signals produced by some species have led to the development of dedicated acoustic detectors (e.g., cod; see Urazghildiiev and Van Parijs 2016). These detectors allow for a more systematic analysis of acoustic data for fish occurrence. Irrespective of species identity, fish choruses can raise ambient sound levels and therefore influence local soundscapes (Erbe et al. 2015).

The biological focus of this study was on marine mammals. Cetacean and pinniped species that may occur in Baffin Bay are listed in Table 1. Marine mammals are the main biological contributors to the underwater soundscape. For instance, fin whale songs can raise noise levels in the 18–25 Hz band by 15 dB for extended durations (Simon et al. 2010). Marine mammals, cetaceans in particular, rely almost exclusively on sound for navigating, foraging, breeding, and communicating (Clark 1990, Edds-Walton 1997, Tyack and Clark 2000). Although species differ widely in their vocal behaviour, most can be reasonably expected to produce sounds on a regular basis. Passive acoustic monitoring is therefore increasingly preferred as a cost-effective and efficient survey method. Seasonal and sex- or age-biased differences in sound production, as well as signal frequency, source level, and directionality all influence the applicability and success rate of acoustic monitoring, and its effectiveness must be considered separately for each species.

Knowledge of the acoustic signals of the marine mammals expected in the study area varies across species. These sounds can be split into two broad categories: Tonal signals, including baleen whale moans and delphinid whistles, and echolocation clicks produced by all odontocetes mainly for foraging and navigating. Although the signals of most species have been described to some extent, these descriptions are not always sufficient for reliable, systematic identification, let alone to design automated detectors to process large data sets (Table 2). For instance, although the whistles of species in the subfamily *Delphininae* (small dolphins) in have been described, the overlap in their spectral characteristics complicates their identification by both analysts and automated detectors (Ding et al. 1995, Gannier et al. 2010). In most cases, baleen whale signals can be reliably identified to the species level, although, seasonal variation in the types of vocalizations produced results in seasonal differences in our ability to detect these species acoustically. For example, the tonal signals produced by blue, fin, and sei whales tend to show lots of similarities in late spring and summer, but they are markedly different from September to April.

Table 1. List of cetacean and pinniped species that may occur in or near the Project area and their Committee on the Status of Endangered Wildlife in Canada (COSEWIC) and Species at Risk Act (SARA) status.

Species	Scientific name	COSEWIC status	SARA status
Cetaceans			
Bowhead whales	*Balaena mysticetus*	Special concern [1]	Not listed [1]
Minke whales	*Balaenoptera acutorostrata*	Not at risk	Not listed
Blue whales	*Balaenoptera musculus*	Endangered	Endangered
Humpback whales	*Megaptera novaeangliae*	Not at risk	Not listed
Beluga whales	*Delphinapterus leucas*	Special concern [2]	Not listed [2]
Narwhal	*Monodon monoceros*	Special concern	Not listed
Killer whales	*Orcinus orca*	Special concern [3]	Not listed [3]
Sperm whales	*Physeter macrocephalus*	Not at risk	Not listed
Northern bottlenose whales	*Hyperoodon ampullatus*	Special concern [4]	Not listed
Pinnipeds			
Ringed seals	*Phoca hispida*	Special concern	Not listed
Bearded seals	*Erignathus barbatus*	Data deficient	Not listed
Harp seals	*Pagophilus groenlandicus*	Not assessed	Not listed
Hooded seals	*Cystophora cristata*	Not at risk	Not listed
Atlantic Walrus	*Odobenus rosmarus*	Special concern [5]	No status [5, 6]

[1] Status of the Eastern Canada-West Greenland population
[2] Status of the Eastern High Arctic-Baffin Bay population
[3] Status of the Northwest Atlantic/Eastern Arctic population
[4] Status of the Status of the Northwest Atlantic/Eastern Arctic population
[5] Status of the High Arctic population
[6] Under consideration for addition

Table 2. Acoustic signals used for identification and automated detection of the species expected in Milne Inlet and supporting references.

Species	Identification signal	Reference
Bowhead whales	Moan	Clark and Johnson (1984) Delarue et al. (2009)
Minke whales	Pulse train	Risch et al. (2013)
Blue whales	A-B vocalization, tonal downsweep	Mellinger and Clark (2003), Berchok et al. (2006)
Humpback whales	Moan, grunt	Dunlop et al. (2008), Kowarski et al. (2018)
Beluga whales	Whistle	Karlsen et al. (2002) Garland et al. (2015)
Narwhal	Whistle, click, buzz, knock	Stafford et al. (2012) Ford and Fisher (1978) Walmsley et al. (2020)
Killer whales	Whistle, pulsed vocalization	Ford (1989) Deecke et al. (2005)
Sperm whales	Click	Watkins (1980)
Northern bottlenose whales	Click	Hooker and Whitehead (2002), Wahlberg et al. (2012)
Ringed seals	Grunt, yelp, bark	Stirling et al. (1987) Jones et al. (2011)
Bearded seals	Trill	Risch et al. (2007)
Harp seals	Grunt, yelp, bark	Terhune (1994)
Walrus	Grunt, knock, bells	Stirling et al. (1987) Mouy et al. (2011)

2. Methods

2.1. Data Acquisition

Underwater sound was recorded using Autonomous Multichannel Acoustic Recorder Generation 4 (AMAR G4, JASCO; Figure 3) in glass spheres. The AMARs were fitted with four M36 omnidirectional hydrophones (GeoSpectrum Technologies Inc., −165 ± 3 dB re 1 V/µPa sensitivity). The hydrophones were protected by a hydrophone cage filled with closed-cell foam to minimize non-acoustic noise caused by water flowing over the hydrophone transducer. This noise is often referred to as 'flow noise'.

The AMARs were deployed in two mooring configurations. The AMAR at AAR1 was deployed on an Autonomous Long-Term Observatory (ALTO)-lander (Figure 3). The AMARs at AAR2 and AAR3, in deeper waters, were deployed using a suspended configuration with the aim of keeping the volumetric array at a planned depth of about 350 m (Figure 4).

The AMAR recorded on a duty cycle of:

- 15 minutes sampled at 16 kHz on all four hydrophones
- 1 minute sampled at 256 kHz on all four hydrophones
- 14 minutes sleep

The total cycle duration was 30 min and the maximum recorded frequency was 128 kHz, which allows capturing all expected sound sources in the area. The recording channels had 24-bit resolution with a spectral noise floor of 32 dB re 1 $\mu Pa^2/Hz$ and a nominal ceiling of 165 dB re 1 µPa. The multichannel data allow for directional analyses of low-frequency (< ~ 1 kHz) sound sources, although these analyses were not part of the scope of this analysis report except to provide the channel orientation information and verify the expected directional performance.

Each recorder was equipped with a Microstrain 3DM-GX5 (HBK, Inc) orientation sensor to track the heading reference of the directional hydrophone arrays. These sensors acquired data once every 50 s.

The AMARs were located at the sites shown in Figure 1 and listed in Table 3. They were deployed between 28 Aug 2022 and 19 Sep 2023.

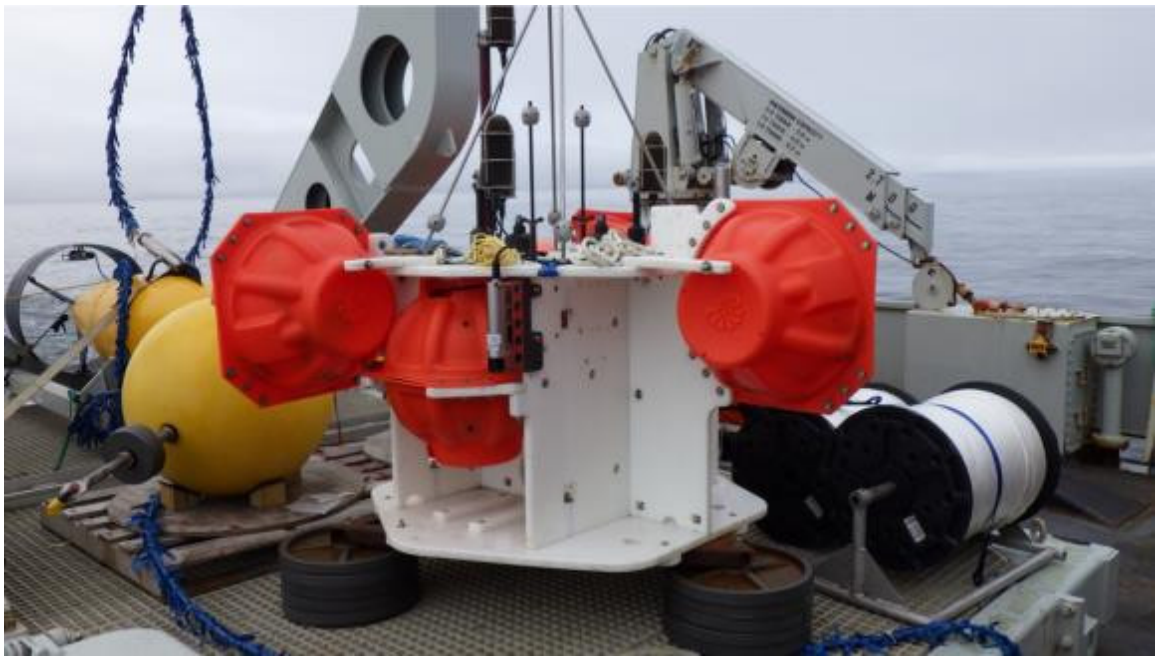

Figure 3. The ALTO-lander configuration (AMAR; JASCO) used to measure underwater sound at station AAR1.

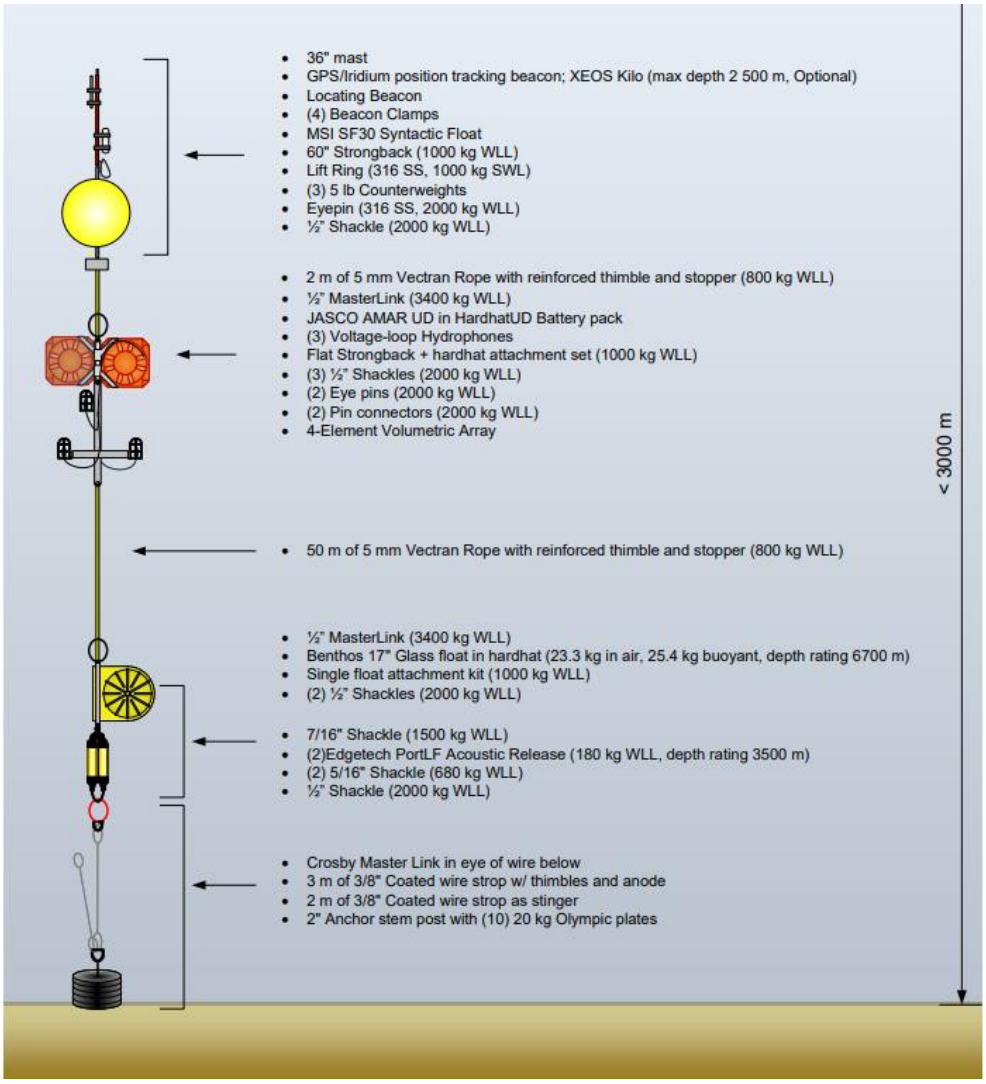

Figure 4. Mooring design used at AAR2 and AAR3.

Table 3. Location and deployment information of the three acoustic recorders deployed between September 2022 and 2023 in this study.

Station ID	Latitude	Longitude	Bottom depth (m)	Recorder depth (m)	Deployment date (UTC)	Deployment time (UTC)	Retrieval date (UTC)
AAR1	72.17537	-72.8229	350	350	28 Aug 2022	21:55:00	19 Sep 2023
AAR2	70.45145	-65.746	1000	~350	29 Aug 2022	19:56:00	18 Sep 2023
AAR3	67.76348	-62.2721	950	~350	31 Aug 2022	0:02:00	17 Sep 2023

2.2. Automated Data Analysis

Each AMAR recovered period collected approximately 6 TB of acoustic data. All acoustic data were processed with JASCO's PAMlab software suite, which processes acoustic data hundreds of times faster than real time. PAMlab performed automated analysis of total ocean noise and sounds from vessels, and marine mammal vocalizations. The following sections describe each type of analysis, and Appendix A provides an overview of the processing algorithms.

2.2.1. Ambient Data Analysis

2.2.1.1. Soundscape and Time Series Analysis

The first stage of the total sound level analysis involves computing the peak sound pressure level (PK) and sound pressure level (SPL) for each minute of data. This reduces the data to a manageable size without compromising its value for characterizing the soundscape (ISO 2017b, Ainslie et al. 2018, Martin et al. 2019). SPL analysis was performed by averaging 120 fast-Fourier transforms (FFTs) that each included 1 s of data with a 50 % overlap that use the Hann window to reduce spectral leakage. The 1 min average data were stored as power spectral densities (1 Hz resolution up to 455 Hz and millidecade frequency bands above 455 Hz) and summed over frequency to calculate decidecade band SPL. Appendix A.2 lists the frequencies of the decidecade bands. (Decidecade bands are similar to 1/3-octave-bands.)

We also applied the millidecade band analysis approach described in Martin et al. (2021). Millidecades are logarithmically spaced frequency bands but have a bandwidth equal to 1/1000th of a decade. Using millidecades instead of 1 Hz frequency bands reduced the size of the spectral data by a large factor without compromising the usefulness of the data.

The decidecade analysis sums as many frequencies as contained in the recorded bandwidth and reduces them to a manageable set of up to 45 bands that approximate the critical bandwidths of mammal hearing. The decade bands further summarize the sound levels into four frequency bands for manageability. Appendices A.1 and A.2 contain detailed descriptions of the acoustic metrics and decidecade analysis, respectively.

In Section 3.1, the total sound levels are presented as:

- **Band-level plots**: These strip charts show the averaged received SPL as a function of time within a given frequency band. We show the total sound levels (across the entire recorded bandwidth from 10–256,000 Hz) and the levels in the decade bands of 8.9–89.1 Hz (Decade A); 89.1–891.3 Hz (Decade B); 891.3–8,913 Hz (Decade C); and 8,913–89,913 Hz (Decade D). The 8.9–89.1 Hz band is generally associated with fin and blue whales, large shipping vessels, flow and mooring noise, and seismic survey impulses. Sounds within the 89.1–891.3 Hz band are generally associated with the physical environment, such as wind and wave conditions, but can also include both biological and anthropogenic sources such as minke and humpback whales, fish, smaller vessels, seismic surveys, and pile driving. Sounds above 1000 Hz include high-frequency components of humpback whale sounds, odontocete whistles and echolocation signals, wind- and wave-generated sounds, and sounds from human sources at close range including pile driving, vessels, seismic surveys, and sonars.

- **Long-term Spectral Averages (LTSAs)**: These color plots show power spectral density levels as a function of time (*x* axis) and frequency (*y* axis). The frequency axis uses a logarithmic scale, which provides equal vertical space for each decade increase in frequency and equally shows the contributions of low- and high-frequency sound sources. The LTSAs are excellent summaries of the temporal and frequency variability in the data.
- **Decidecade box-and-whisker plots**: The 'boxes' in these figures represent the middle 50 % of the range of SPL, so that the bottom of the box is the sound level 25th percentile (L_{25}) of the recorded levels, the bar in the middle of the box is the median (L_{50}), and the top of the box is the level that exceeded 75 % of the data (L_{75}). The whiskers indicate the maximum and minimum ranges of the data.
- **Spectral density level percentiles**: While the decidecade box-and-whisker plots represent the histogram of each band's sound pressure levels, the power spectral density data have too many frequency bins for a similar presentation. Instead, colored lines represent the L_{eq}, L_5, L_{25}, L_{50}, L_{75}, and L_{95} percentiles of the histograms. Shading underneath these lines indicates the relative probability distribution. It is common to compare the power spectral densities to the results from Wenz (1962), which documented the variability of ambient spectral levels off the US Pacific coast as a function of the frequency of measurements for a range of weather, vessel traffic, and geologic conditions (see Figure 2). The Wenz levels are only appropriate for approximate comparisons because those data were collected in deep water, largely before an increase in low-frequency sound levels (Andrew et al. 2011).

2.2.2. Vessel Detection

The boat and ship detectors compare sound levels in established frequency range to criteria values. Boats (small vessels) and ships (large vessels) can be distinguished because boats are quieter and emit more sound at higher frequencies than ships. The highest sound level within the minutes flagged as having a vessel present is assigned as the closest point of approach (CPA). The criteria values are outlined in Table 4. Criteria names are shown in italics in the following descriptions:

- The background SPL within the frequency range is calculated as a long-term average over the *Background window duration*.
- Each minute's SPL (within the frequency range) must be greater than the background value by the *Shipping to background threshold*.
- Each minute's SPL (within the frequency range) must exceed the total broadband SPL by the *Shipping to RMS Threshold.*
- Each minute's SPL must be greater than the *Minimum broadband SPL.*
- The average number of tonals detected over a *Minimum shipping duration* minute window must be greater than *Minimum number of shipping tonals.*
- The duration of the shipping detection must be greater than *Minimum shipping duration* and less than *Maximum shipping duration.*

The vessel detection process is illustrated in Figure 5. Once vessels are detected, we then defined a "anthropogenic shoulder" 15-min before and after each detection. These periods did not meet the detector's criteria but contained acoustic energy from the detected vessels and were therefore excluded from the data used to characterize ambient sound.

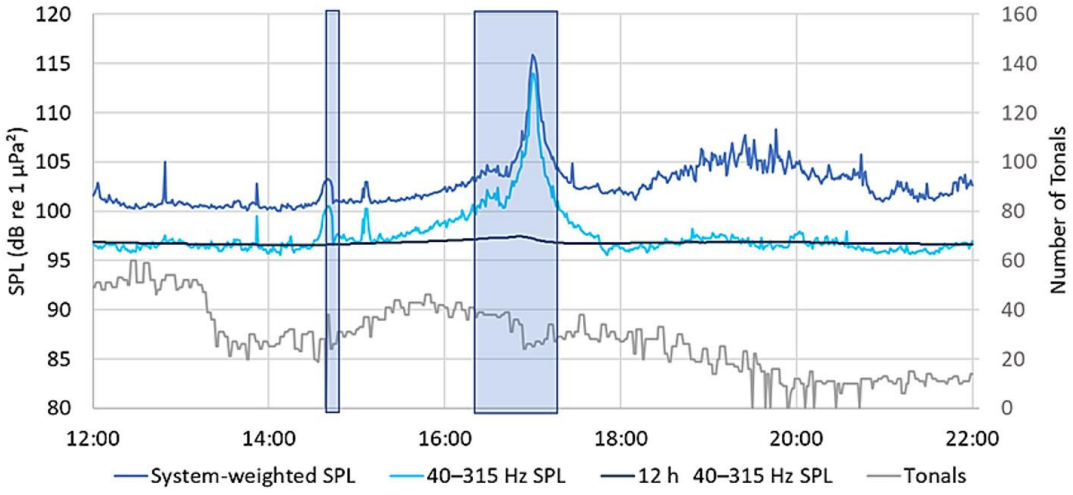

Figure 5. Example of broadband and 40–315 Hz band sound pressure level (SPL), as well as the number of tonals detected per minute as a vessel approached a recorder, stopped, and then departed. The shaded area is the period of shipping detection. Fewer tonals are detected at the ship's closest point of approach (CPA) at 17:00 because of masking by broadband cavitation noise and due to Doppler shift, which affects the tone frequencies.

Table 4. Parameters of the boat and ship detector.

Detector	f_{min} flag (Hz)	f_{max} flag (Hz)	Min. broadband SPL (dB)	Min. # of shipping tonals	Background window duration (min)	Shipping duration (min)		Typical shipping passing duration (min)	Shipping to background threshold (dB)	Shipping to rms threshold (dB)	Anthropogenic shoulder (min)
						Min.	Max.				
Ship	40	315	105	3	720	5	360	30	3	12	15
Boat	315	2000	95	0.49	720	3	60	10	3	15	15

2.2.3. Marine Mammal Detection Overview

We used a combination of automated detector-classifiers and manual review by experienced analysts to determine the presence of sounds produced by marine mammals in the acoustic data. Given the limited effort allocated to manual analysis in this study, we tailored the manual data review to maximize encounter rates with priority species indicated by DRDC. These species were killer whales, northern bottlenose whales, and sperm whales.

First, a suite of automated detectors was applied to the full data set (see Appendices B.1 and B.2). Second, a subset of acoustic data was selected for manual review of automated detector results. The review samples were selected via our Automatic Data Selection for Validation (ADSV) algorithm (Kowarski et al. 2021) (see Appendix B.3). Calls from all species manually detected in these files were annotated. We reviewed 1 % of the 16-kHz data recorded from 28 Aug until 14 Nov 2022 and from 15 Jun until 19 Sep 2023 for killer and sperm whale presence, focusing the effort on the ice-free season (but incorporating ice formation and break up) when these two species are most likely to be present. We also reviewed 0.5 % of the 256 kHz data for presence of northern bottlenose whale clicks. Finally, automated detector performance metrics were calculated (see Appendix B.4) and hourly marine mammal occurrence plots that incorporated manual and automated detections were created (see Section 3.2). Where automated detector results were below our performance thresholds or did not add additional information to species occurrence, only the validated results from manual analysis are presented. These marine mammal analysis steps are summarized here and detailed in Appendix B.

2.2.3.1. Automated Click Detection

Odontocete clicks are high-frequency impulses ranging from 1 to over 150 kHz (Au et al. 1999, Møhl et al. 2000). We applied an automated click detector to the 256 kHz data (audio bandwidth up to 256 kHz for 1 min of every 30 min) to identify clicks from sperm whales, beaked whales, porpoises, and delphinids. This automated detector is based on zero-crossings in the acoustic time series. Zero-crossings are the rapid oscillations of a click's pressure waveform above and below the signal's normal level. Zero-crossing-based features of automatically detected events are then compared to templates of known clicks for classification (see Appendix B.1 for details).

2.2.3.2. Automated Tonal Signal Detection

Tonal signals are narrowband, often frequency-modulated, signals produced by many species across a range of taxa (e.g., baleen whale moans, delphinid whistles). They range predominantly between 15 Hz and 20 kHz (Berchok et al. 2006, Risch et al. 2007), thus automated detectors for these species were applied to the 16 kHz data. The automated tonal signal detector identified continuous contours of elevated energy and classified them against a library of marine mammal signals (see Appendix B.2 for details).

2.2.3.3. Automated Detector Validation

JASCO's suite of automated detectors are developed, trained, and tested to be as reliable and broadly applicable as possible. However, the performance of marine mammal automated detectors varies across acoustic environments (e.g., Hodge et al. 2015, Širović et al. 2015, Erbs et al. 2017, Delarue et al. 2018). Therefore, automated detector results must always be supplemented by some level of manual review to evaluate automated detector performance. Here, we manually analyzed a subset of acoustic files for the presence/absence of marine mammal acoustic signals via spectrogram review in JASCO's PAMlab software. A subset of acoustic data, consisting of 104 256-kHz (0.5%) and 174 16-kHz (1%) files at each station, was selected via ADSV for manual review (see Appendix B.3).

To determine the performance of the automated detectors, the automated and manual results (excluding files where an analyst indicated uncertainty in species occurrence) were fed into an algorithm that calculates precision (*P*), recall (*R*), and Matthew's Correlation Coefficient (*MCC*) (see Appendix B.4 for formulas). *P* represents the proportion of files with detections that are true positives. A *P* value of 0.90 means that 90 % of the files with automated detections truly contain the targeted signal, but it does not indicate whether all files containing acoustic signals from the species were identified. *R* represents the proportion of files containing the signal of interest that were identified by the automated detector. An *R* value of 0.90 means that 90 % of files known to contain a target signal had automated detections, but it says nothing about how many files with automated detections were incorrect. An MCC is a combined measure of *P* and *R*, where an MCC of 1.00 indicates perfect performance, i.e., all events were correctly automatically detected. The algorithm determines a per-file automated-detector threshold (the number of automated detections per file at and above which automated detections were considered valid) that maximizes the MCC.

For many species, more than one automated detector targeted their vocalizations. In these instances, the performances of all automated detectors were evaluated, and the highest performing detector was used to represent species/vocalization-type occurrence in Section 3.2. Only automated detections associated with a *P* greater than or equal to 0.75 were considered. When *P* was less than 0.75, only the validated results were used to describe the acoustic occurrence of a species.

JASCO's Ark software was used to plot the occurrence of each species (both validated and automated, or validated only where appropriate) as time series showing the hourly presence/absence over each day of the recording period. Automated detector performance metrics associated with the results should be considered when interpreting result.

3. Results

3.1. Ambient Sound

The results of the soundscape characterization are presented in Figures 6 and 7 as well as Table 5. They reveal a picture consistent with observations from other Arctic areas where sound levels generally decrease during the ice-covered season when the water column is isolated from wind and wave-induced noise. We noted a latitudinal trend in sound levels, with median broadband levels being 6 dB higher at AAR3 compared to AAR1. This latitudinal spread in sound levels was present for each of the decade bands but was most pronounced for the 10–100 Hz band. It is possible that the higher levels in this band at AAR2 and AAR3 were due to the suspended mooring used at these sites and flow noise caused by strumming cables. Alternatively, or additionally, greater vessel traffic or closer proximity to areas of denser traffic as one moves farther south could also drive some of the higher levels at AAR2 and AAR3.

No data quality issues were noted with the acoustic data. All three acoustic recorders performed as expected for the planned duration of the study.

We noted variable tones above 10 kHz in the acoustic data recorded at AAR3 from mid-December 2022 onward (Figure 6), which contrast with the flat lines seen on the LTSA above 10 kHz at AAR1 and AAR2 that are attributed to the CTD. This points to a potential malfunction of the CTD installed on the mooring deployed at AAR3.

The readings from the 3DM-GX5 orientation sensors are plotted as time series in Figure 8. As expected, the suspended moorings at AAR2 and AAR3 showed more variability in yaw than the bottom-mounted ALTO at AAR1. A closer look at the variations in yaw at AAR3 suggest a potential influence of tidal currents in the variations in orientation (Figure 9). Yaw was more variable at AAR3 than at AAR2, possibly indicating more current at AAR3. The sensor orientation remained stable at AAR2 but changed by ~ 50° at AAR3. While one would have expected no change in orientation at AAR3, the bottom-mounted ALTO rotated by ~ 18° over the course of the deployment. The relative amount of movement at AAR3 compared to the other locations is consistent with the additional low frequency sound levels at this station.

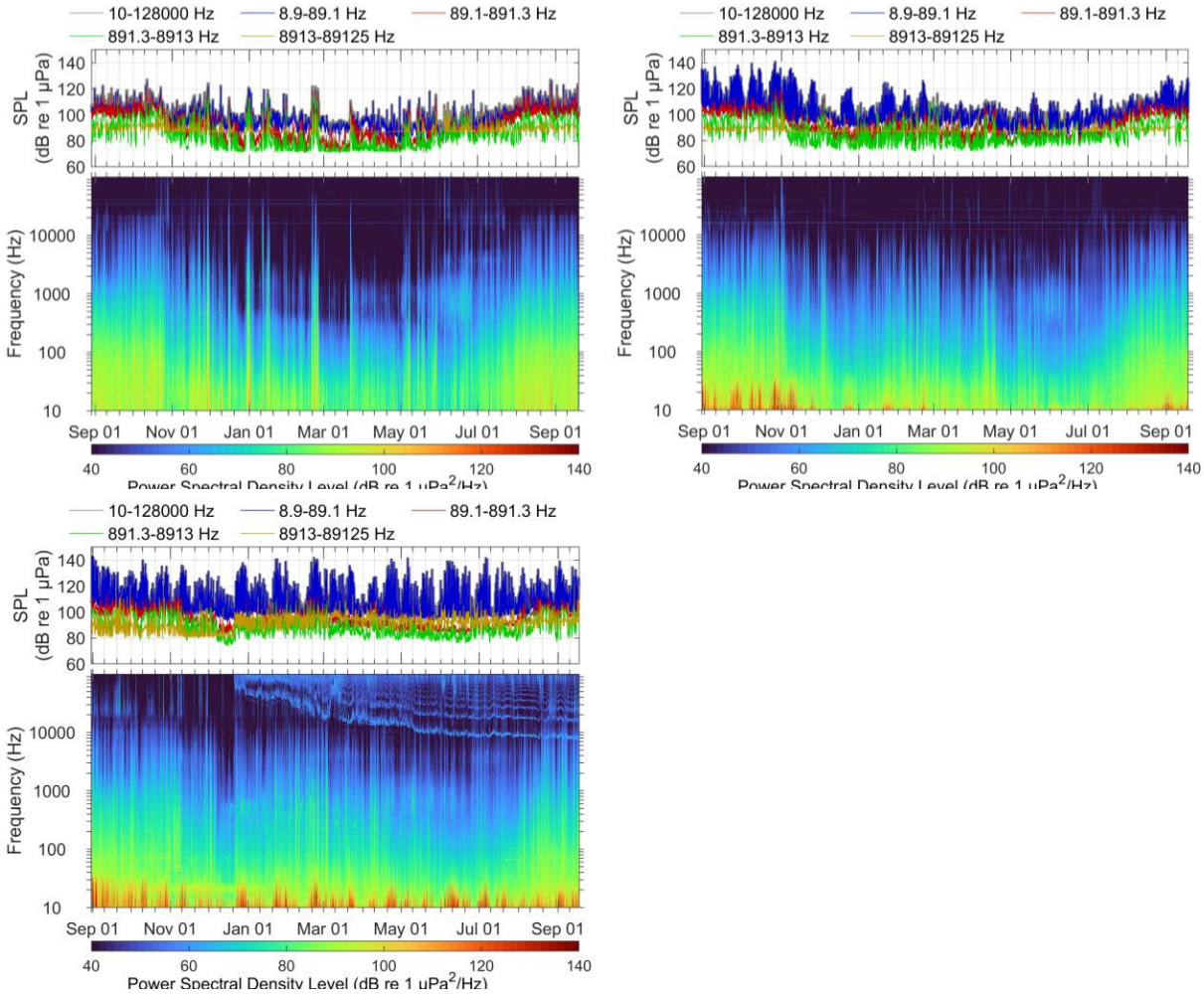

Figure 6. (Top panel) In band sound pressure level and (bottom panel) long term spectrogram of received sound recorded between 29 Aug 2022 and 19 Sep 2023 at stations (top left) AAR1, (top right) AAR2, and (bottom) AAR3 for the duration of the deployment for channel 1.

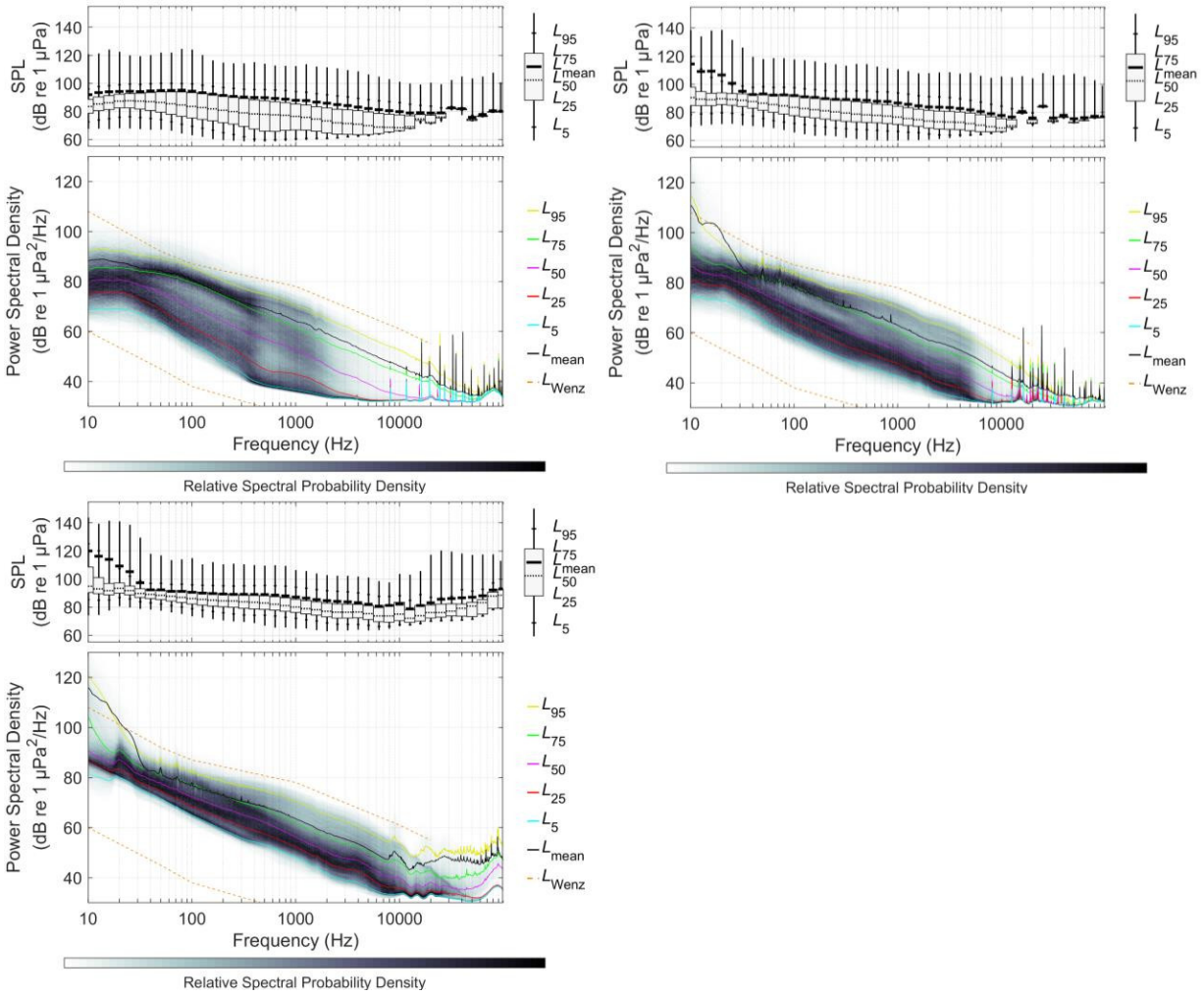

Figure 7. (Top panel) Decidecade boxplot showing the distribution of Sound pressure level within a decidecade band and (bottom panel) power spectral density percentile plot showing the distribution of received levels as a function of frequency for data recorded between 29 Aug 2022 and 19 Sep 2023 at stations (top left) AAR1, (top right) AAR2, and (bottom) AAR3 for the duration of the deployments for channel 1.

Table 5. Band sound level statistics between 10 and 128000 Hz over the full deployment for each of the recorders.

Sound level statistic	10–128000 Hz			8.9–89.1 Hz			89.1–891.3 Hz			891.3–8913 Hz			8913-89125 Hz		
	AAR1	AAR2	AAR3	AAR1	AAR2	AAR3	AAR1	AAR2	AAR3	AAR1	AAR2	AAR3	AAR1	AAR2	AAR3
Min	88.6	89.1	93.2	77.6	81.1	81.3	70.3	73.6	76.3	70.9	71.2	72.6	86.8	86.6	82
L_5	90.4	92.3	99.1	85	88.9	94.7	75.4	80.4	85.2	71.3	74.5	78.7	87.1	86.9	82.3
L_{25}	93.7	96.6	102.3	91.2	94.9	98.7	82.3	85.3	89.7	74.9	79	82.9	87.2	87	88.6
L_{50}	98.9	101.4	105.6	96.9	100	102.9	90.8	90.8	94.1	83.3	84	86.8	87.4	87.2	93.6
L_{75}	105.7	107.3	111.5	102.9	105.3	110.4	100.8	99.6	99.2	92.1	91.4	92.6	89	87.9	95.8
L_{95}	111.6	120.4	126.8	109.2	120.2	126.8	106.9	105.7	105.3	101	100.7	101.1	93.2	91.1	99.7
Max	130.8	143.6	146.5	156.8	145.5	149.9	135.5	128.8	129.5	123.6	120.3	117.3	112.4	114.2	126.8
Mean	106.5	117.1	122.5	106.9	117.2	122.6	101.4	99.7	99.3	94.9	93.6	94.1	89.7	88.8	96.6

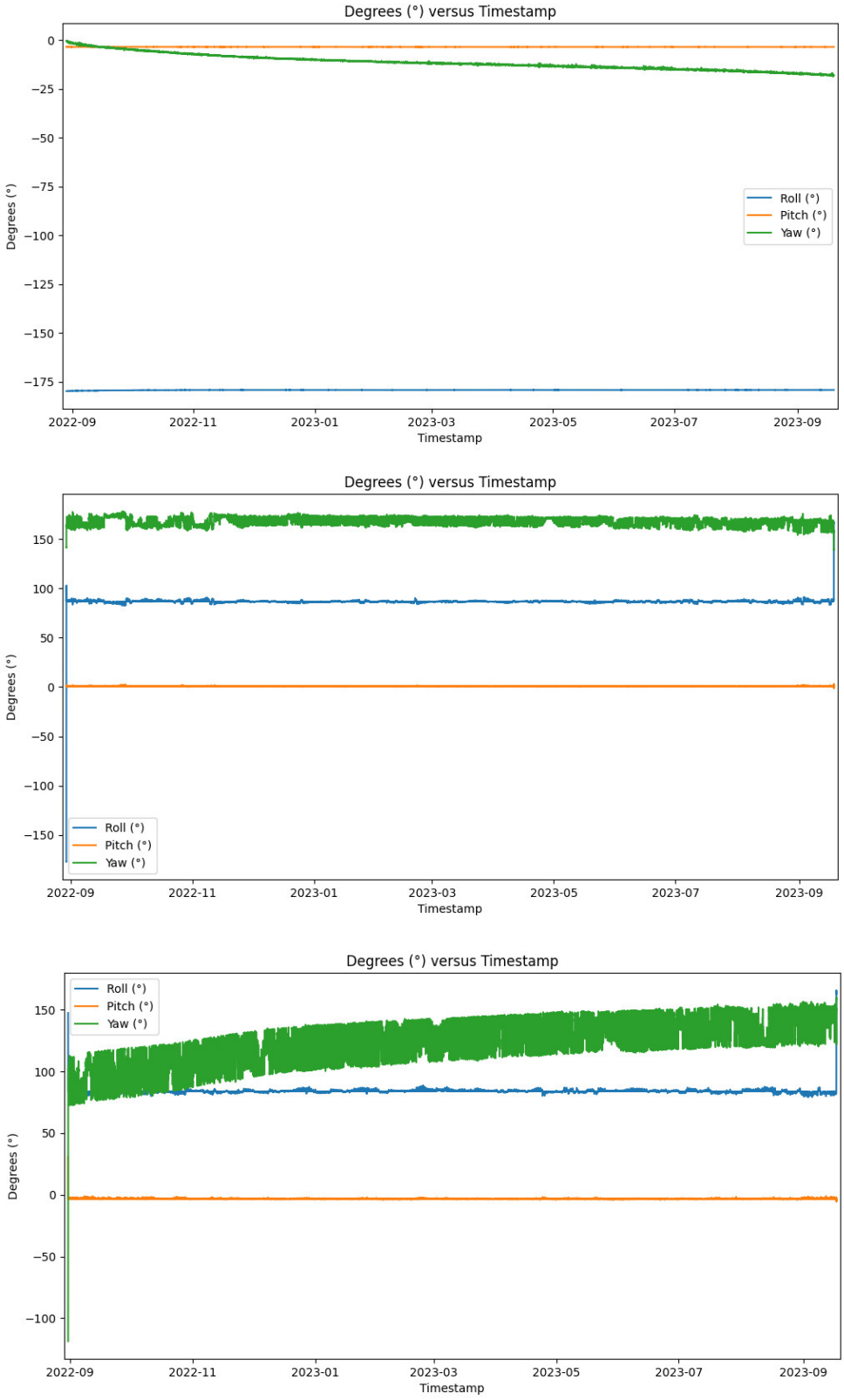

Figure 8. Time series of pitch, roll and yaw readings from 3DM-GX5 orientation sensor installed on the moorings deployed at AAR1 (top), AAR2 (middle) and AAR3 (bottom) from 28 August 2022 until 19 September 2023.

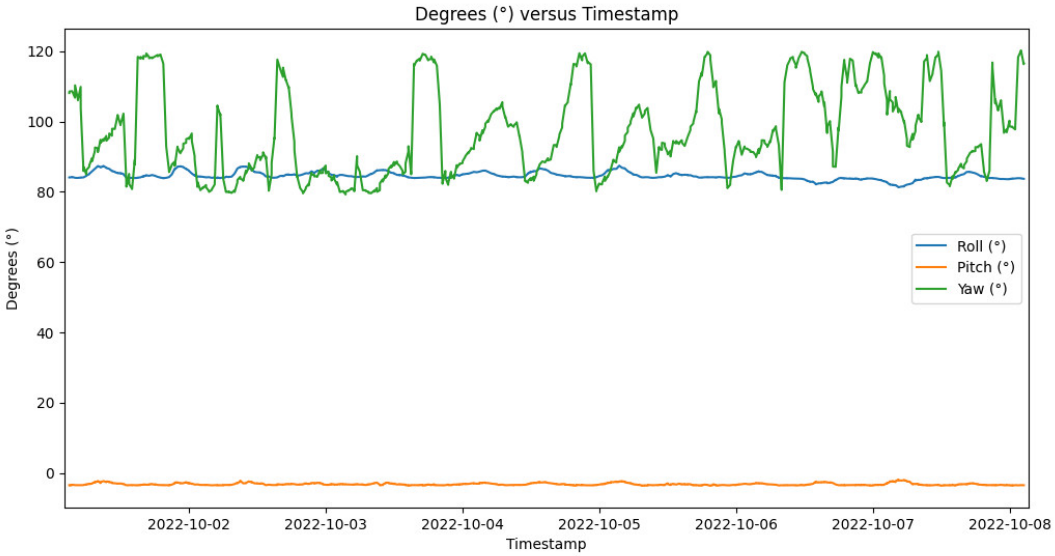

Figure 9. Time series of pitch, roll and yaw readings from 3DM-GX5 orientation sensor installed on the mooring deployed at AAR3 between 1 and 8 October 2022.

3.2. Vessel Detections

Vessels were automatically detected at all stations and are shown in relation to sea ice cover in Figure 10. The bulk of detections occurred, as expected, during the ice-free season. The sporadic detections occurring during periods of heavy ice cover are presumably false detections although we cannot rule out the occasional passage of a vessel. Indeed, sounds caused by sea ice can be similar to the long tones produced by vessels and that the detector is targeting.

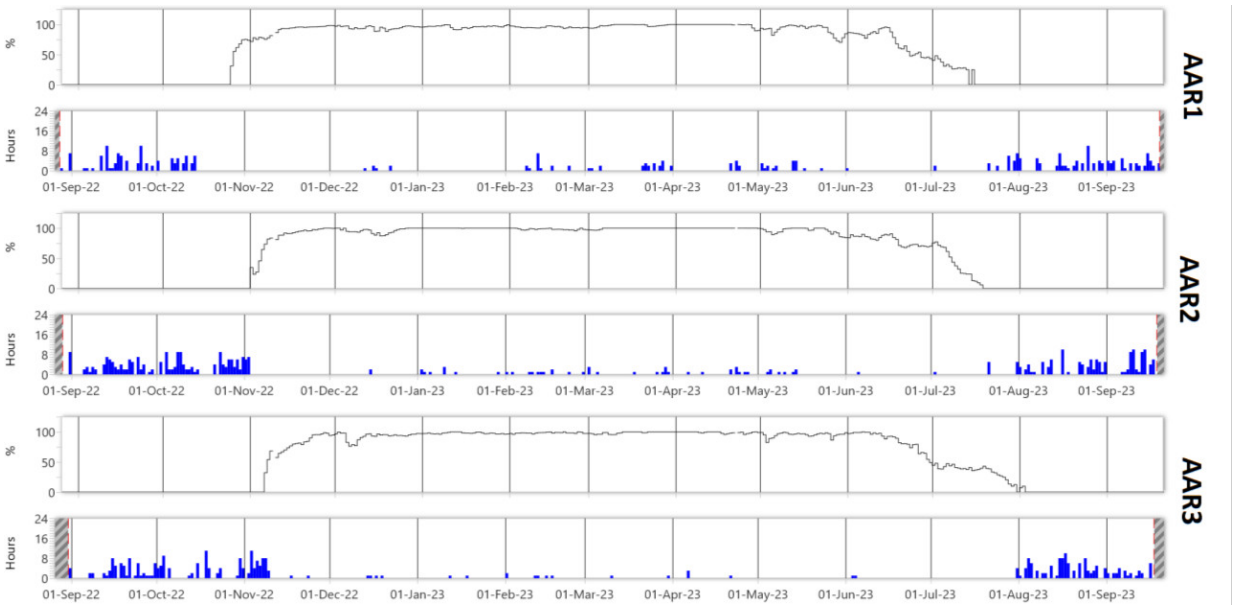

Figure 10. Sea ice concentration (%; top panel) and daily number of hours with vessel detections (bottom panel) at each monitoring location (AAR1, AAR2, and AAR3) between 28 Aug 2022 and 19 Sep 2023.

3.3. Marine Mammals

The acoustic presence of marine mammals was identified automatically by JASCO's detectors (see Section 2.2.3.3) and via the manual data review of a subset of data (see Section 2.2.3). The following species were detected in the acoustic data: blue, fin, bowhead, killer, narwhal, sperm, and northern bottlenose whales as well as bearded and harp seals. Beluga whales, pilot whales, and an unidentified species of dolphins may have been present but additional analysis would be required to confirm their occurrence.

Table 6 presents the performance metrics of the automated detectors exceeding our acceptance thresholds (see Section 2.2.3.3). The manual validation samples were built based on the outputs of the detectors targeting the species of interest to DRDC (killer whales, northern bottlenose whales, and sperm whales) to maximize encounter rates with the calls of these species given the limited review effort available. As a result, the ADSV are not representative of the data sets for other species and therefore not adequate to evaluate detector performance. The exclusion of 16 kHz data recorded during the ice-covered period from the pool of files available for review also automatically reduced the number of calls from ice-associated species (e.g. bowhead whale and bearded seal, at a minimum) that could be used to assess the detector performance. It is expected that the manual review of all 16 kHz data (i.e., including the 15 Nov to 15 Jun period) when bowhead whales and bearded seals are most common would provide

ample data to validate and use the output of the detectors targeting their calls (which were applied to the data).

The northern bottlenose whale was the only target species whose signals were abundant enough (at AAR2 and AAR3) for the corresponding click detector to be evaluated and automated detections used to characterize their occurrence. Fin whale 20-Hz pulses and narwhal clicks, although non-target signals, were also abundant enough during specific periods for automated detections to be used to describe their occurrence (Table 6).

The results presented in the following sections provide a minimum estimate of occurrence, particularly for those species that were only assessed manually. For context and because the distribution of most species is affected by sea ice (either through affinity or avoidance), acoustic detections are plotted as time series in relation to sea ice concentrations at the location of the recorders. All sea ice data were procured via the EUMETSAT Ocean and Sea Ice Satellite Application Facility (https://osi-saf.eumetsat.int/products/osi-450).

Table 6. Automated detector performance including the threshold implemented (minimum number of automated detections per file for species to be considered present), the detector precision (*P*), recall (*R*) and MCC score after any exclusion period and/or threshold restrictions have been applied. The data set (sampling rate) for which the automated detector performance was calculated is provided. This table only includes species for which precision exceeded a threshold of 0.75. N: Number of files manually reviewed; TP: True positive; FP: False positive; FN: False negative; TN: True negative.

Species/group (sampling rate)	Station	Automated detector	Exclusion period	Per-file threshold	*N*	*P*	*R*	*MCC*	*TP*	*FP*	*FN*	*TN*
Fin whale 20-Hz pulse (16 kHz)	AAR3	Atl_FW_21	15 Nov to 15 Sep 2022	6	171	1.00	0.74	0.80	42	0	15	96
Northern bottlenose whale clicks (256 kHz)	AAR2	NBW:Click	25 Oct 2022 to 20 Aug 2023	1	100	1	1	1	11	0	0	93
	AAR3		1 Nov 2022 to 13 Jul 2023	36	104	1.00	0.96	0.97	22	0	1	77
Narwhal clicks (256 kHz)	AAR1	UDA.Click	None	264	105	1.00	0.25	0.49	1	0	3	62
	AAR2	AWSD_La.Click	29 Aug to 27 Oct 2022	10	100	0.91	0.77	0.81	10	1	3	82
	AAR3	Narwhal.Click	31 Aug to 31 Oct 2022	204	104	1.00	0.50	0.64	9	0	9	43

3.3.1. Blue Whale

Blue whale A-B song notes (17 Hz tones in Figure 11) were detected once at AAR3 on 31 Aug 2023.

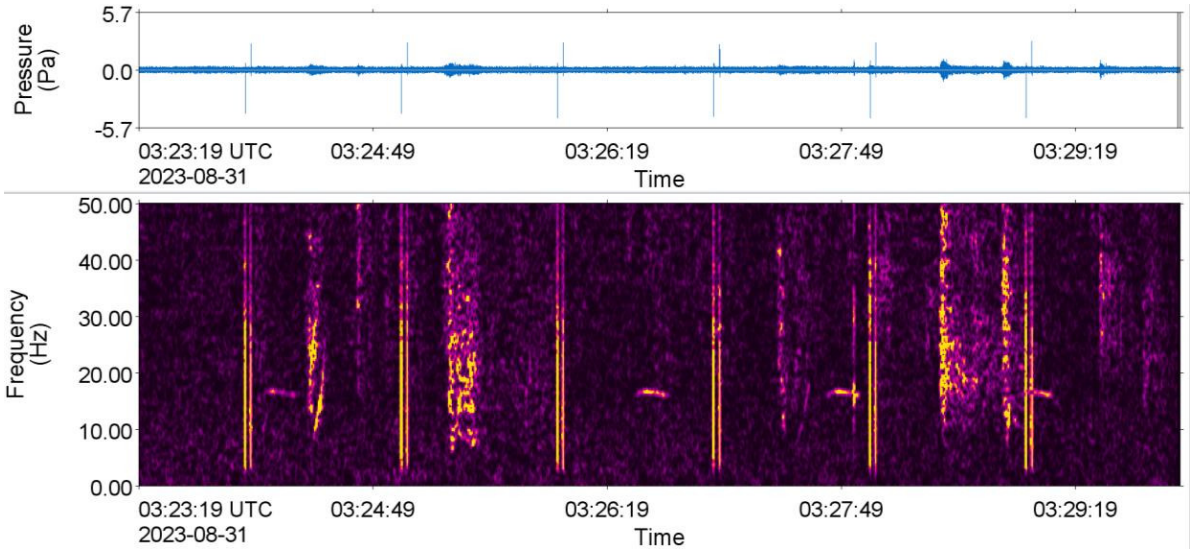

Figure 11. Blue whale: Spectrogram of A-B notes recorded at AAR3 on 31 August 2023 (0.4 Hz discrete Fourier Transform (DFT) frequency step, 2 s DFT temporal observation window (TOW), 0.5 s DFT time advance, and Hann window). The spikes are from the ADCP.

3.3.2. Fin Whale

Fin whale 20-Hz and 130-Hz notes (Figure 12) were detected at all stations but most commonly at AAR3 (Figure 13). The manual detections at AAR1 and AAR2 presumably underestimate the true occurrence of this species, but it is worth noting that fin whales were detected late during the open-water season and, in fact, shortly before sea ice formation in 2022. The abrupt end of detections in Figure 13 is an artefact of the exclusion period imposed on the automated detections to match manual detections. The striation pattern observed with detections at AAR3 in fall 2022 is presumably caused by variations in background noise, and therefore masking, due to tidal currents.

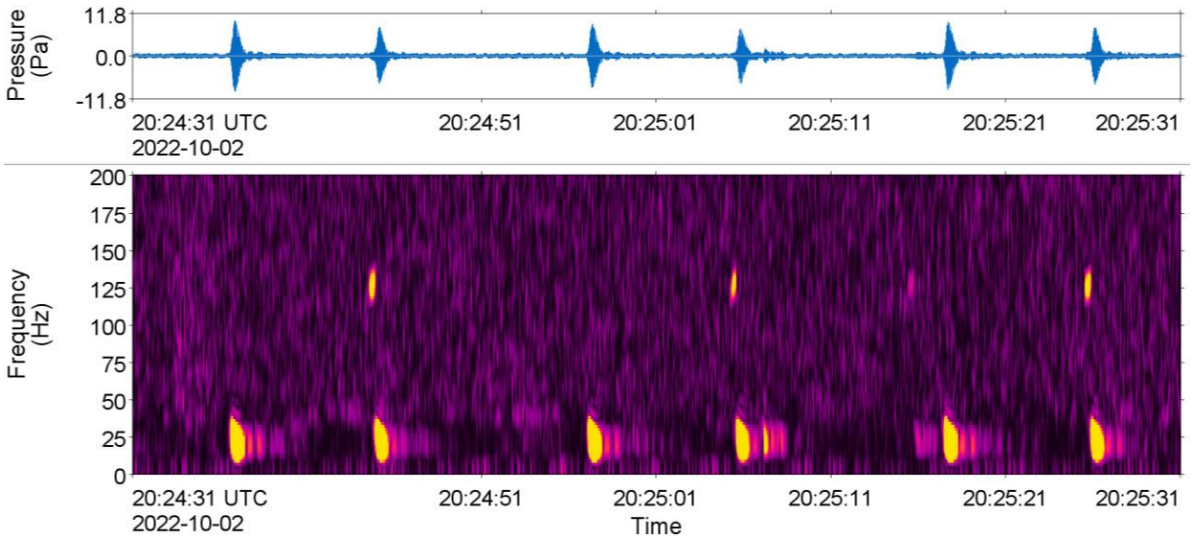

Figure 12. Fin whale: Spectrogram of 20-Hz and 130-Hz notes recorded at AAR3 on 2 Oct 2022 (2 Hz discrete Fourier Transform (DFT) frequency step, 0.125 s DFT temporal observation window (TOW), 0.03125 s DFT time advance, and Hann window). The spectrogram is 60 s long.

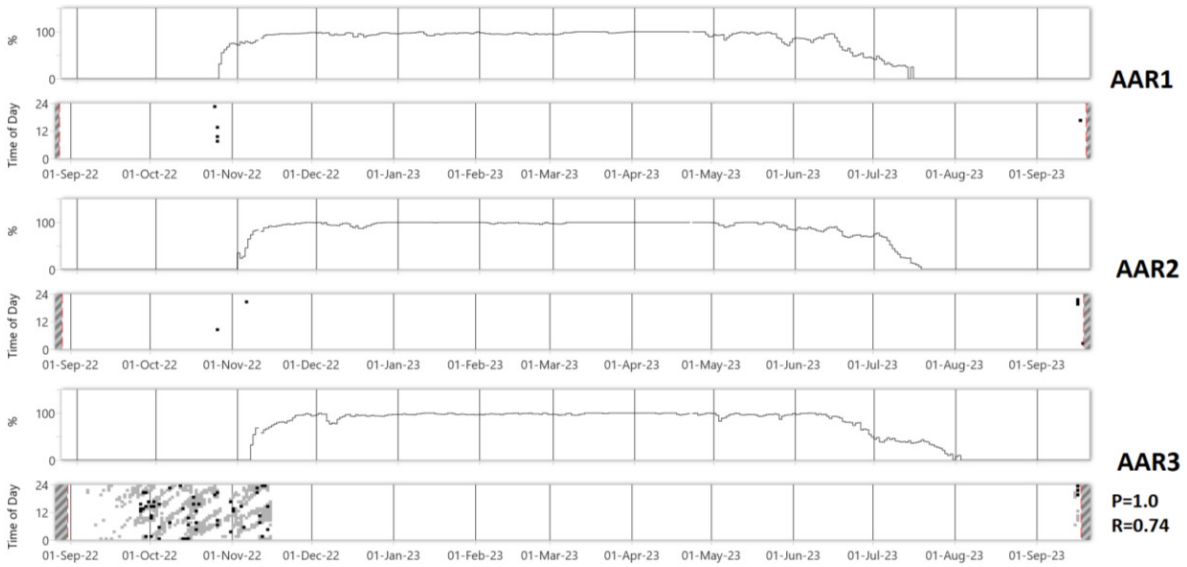

Figure 13. Fin whale: Daily time series of sea ice concentration (%; top panel) and hourly presence of manual (black squares) and automated (grey squares) detections (bottom panel) at each monitoring location (AAR1, AAR2, and AAR3) between 28 Aug 2022 and 19 Sep 2023. Sea ice concentration data from EUMETSAT Ocean and Sea Ice Satellite Application Facility, Global sea ice concentration climate data record 1979-2015 (v2.0, 2017), OSI-450, doi: 10.15770/EUM_SAF_OSI_0008, accessed 6 March 2024.

Bowhead Whale

Bowhead whale vocalizations (Figure 14) were recorded at all stations. Detections occurred most frequently in the second half of June but continued into July at all stations. Detections also occurred around ice formation at AAR1 and from late December to early February in 100 % ice concentrations at AAR3 (Figure 15).

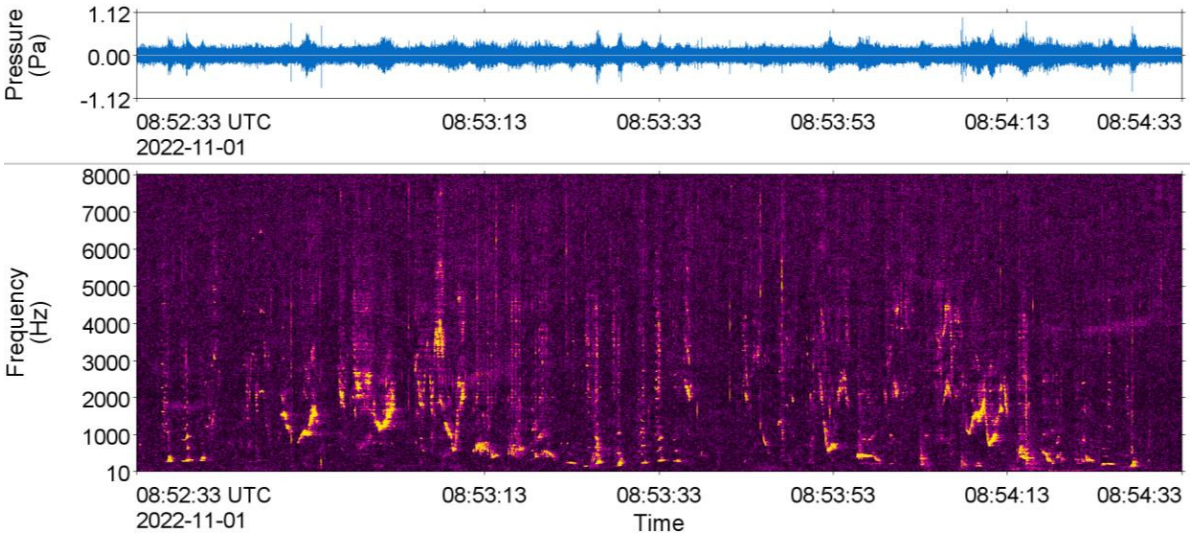

Figure 14. Bowhead whale: Spectrogram a fragment of song recorded at AAR1 on 1 Nov 2022 (2 Hz discrete Fourier Transform (DFT) frequency step, 0.125 s DFT temporal observation window (TOW), 0.03125 s DFT time advance, and Hann window). The spectrogram is 2 min long.

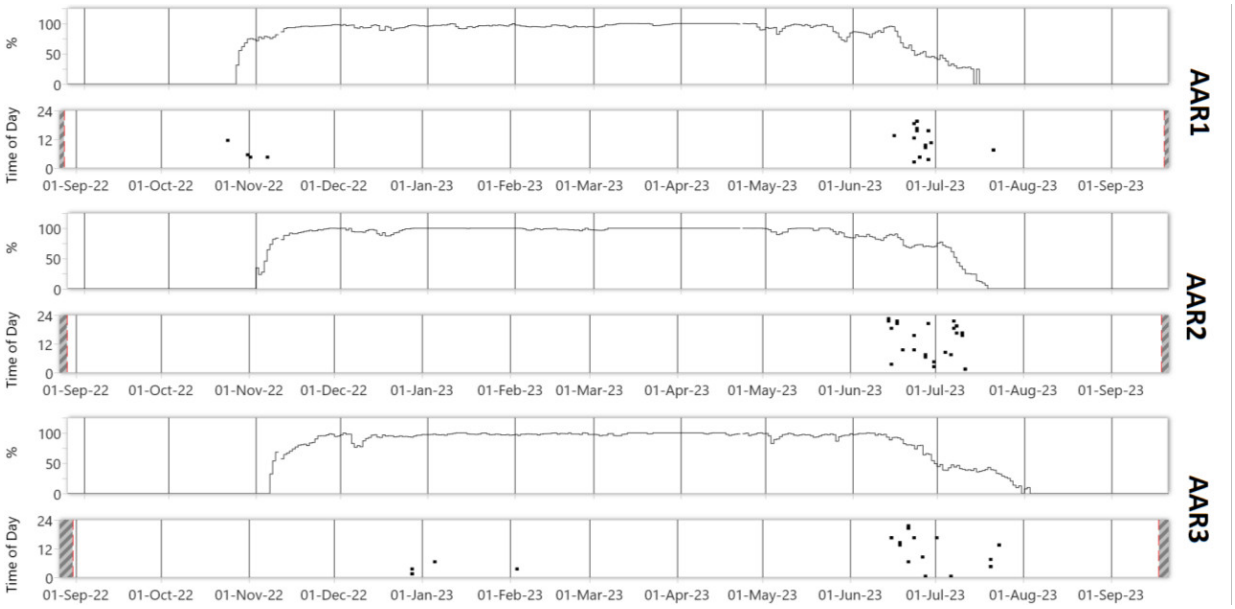

Figure 15. Bowhead whale: Daily time series of sea ice concentration (%; top panel) and hourly presence of manual detections (bottom panel) at each monitoring location (AAR1, AAR2, and AAR3) between 28 Aug 2022 and 19 Sep 2023. Sea ice concentration data from EUMETSAT Ocean and Sea Ice Satellite Application Facility, Global sea ice concentration climate data record 1979-2015 (v2.0, 2017), OSI-450, doi: 10.15770/EUM_SAF_OSI_0008, accessed 6 March 2024.

3.3.4. Killer Whale

Killer whale vocalizations (Figure 16) were detected at all stations, exclusively during ice-free periods (Figure 17). Because the occurrence results presented here are based on the manual review of a limited amount of data, they have to be interpreted cautiously. We note, however, a greater density of detections at AAR1 (shallower and closer to shore than the other stations) in fall 2022 and the sequential timing of the first detections in 2023 from south (AAR3) to north (AAR1).

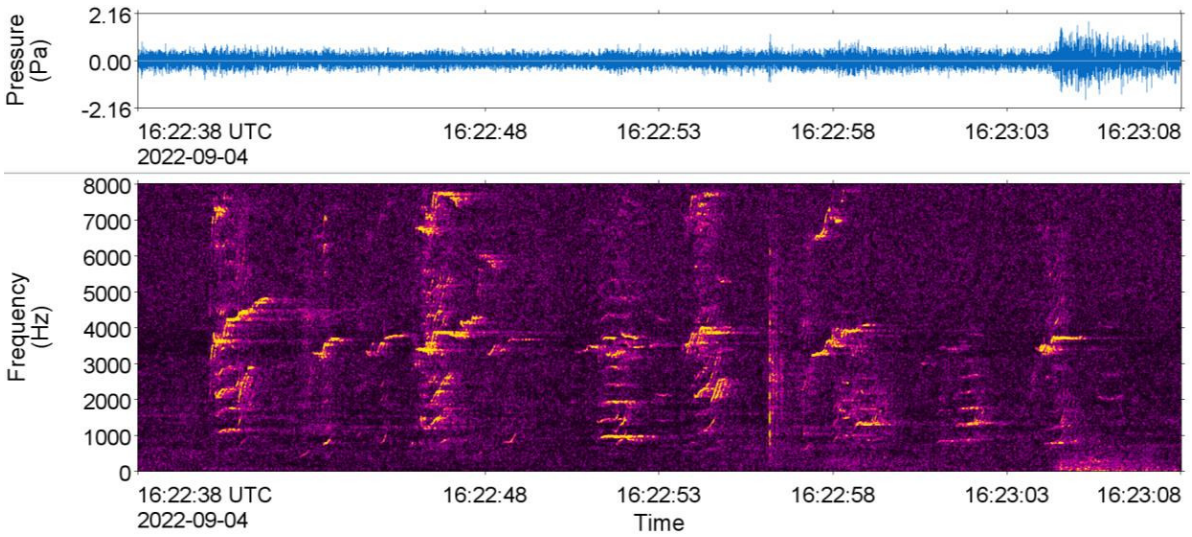

Figure 16. Killer whale: Spectrogram of pulsed calls recorded at AAR1 on 4 Sep 2022 (4 Hz discrete Fourier Transform (DFT) frequency step, 0.05 s DFT temporal observation window (TOW), 0.01 s DFT time advance, and Hann window). The spectrogram is 30 s long.

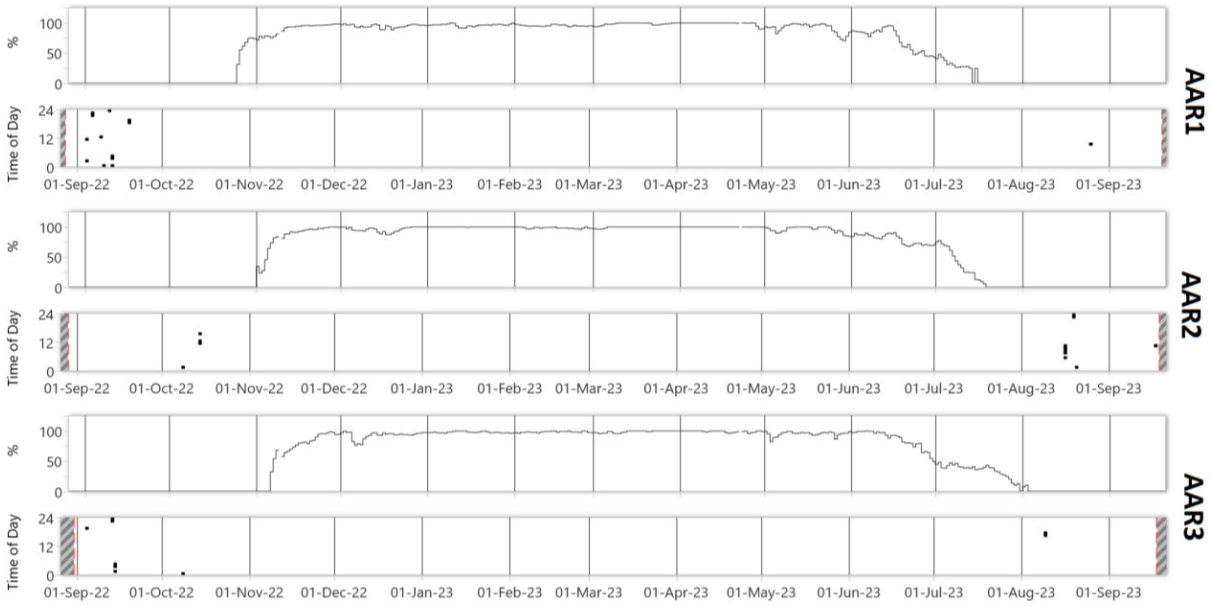

Figure 17. Killer whale: Daily time series of sea ice concentration (%; top panel) and hourly presence of manual detections (bottom panel) at each monitoring location (AAR1, AAR2, and AAR3) between 28 Aug 2022 and 19 Sep 2023. Sea ice concentration data from EUMETSAT Ocean and Sea Ice Satellite Application Facility, Global sea ice concentration climate data record 1979-2015 (v2.0, 2017), OSI-450, doi: 10.15770/EUM_SAF_OSI_0008, accessed 6 March 2024.

3.3.5. Northern Bottlenose Whale

Northern bottlenose whale clicks (Figure 18) were detected at AAR2 and AAR3 (Figure 19). This species was present until ice formation in fall 2022 at both stations. Detections resumed when sea ice cover was declining but still present at AAR3 around mid-July. At AAR2, detections did not resume until late August 2023. It should be noted, however, that automated detections were temporally restricted on the basis of manual detections (see exclusion periods in Table 6) and that additional manual data review could reveal earlier detections at AAR2 in 2023 and a longer detection period in the fall, even though this species is not generally known to associate with sea ice.

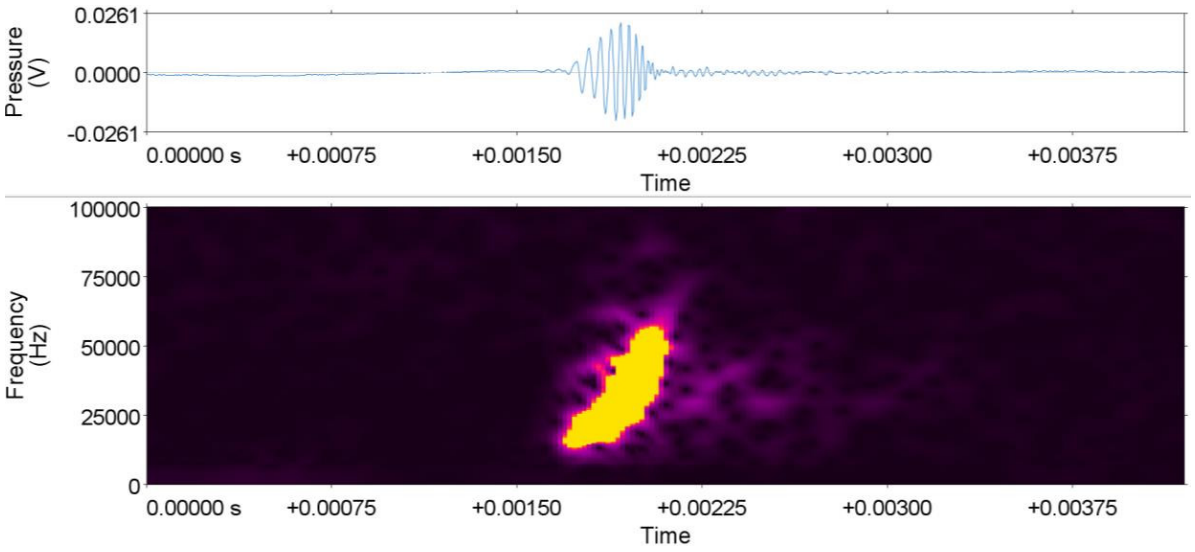

Figure 18. Northern bottlenose whale: Spectrogram of a click recorded at AAR3 on 25 Sep 2022 (512 Hz discrete Fourier Transform (DFT) frequency step, 0.26 ms DFT temporal observation window (TOW), 0.02 ms DFT time advance, and Hann window). The spectrogram is 4 ms long.

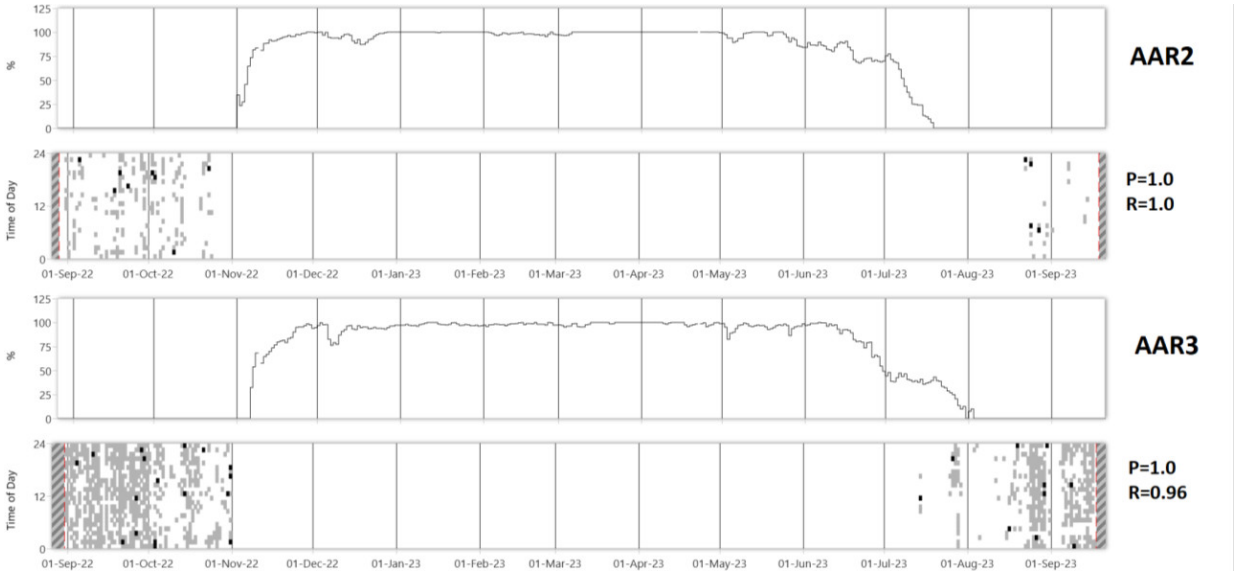

Figure 19. Northern bottlenose whale: Daily time series of sea ice concentration (%; top panel) and hourly presence of manual (black squares) and automated (grey squares) detections (bottom panel) at each monitoring location (AAR1, AAR2, and AAR3) between 28 Aug 2022 and 19 Sep 2023. The performance metrics of the detector are shown for each station. Sea ice concentration data from EUMETSAT Ocean and Sea Ice Satellite Application Facility, Global sea ice concentration climate data record 1979-2015 (v2.0, 2017), OSI-450, doi: 10.15770/EUM_SAF_OSI_0008, accessed 6 March 2024.

3.3.6. Sperm Whale

Sperm whale clicks (Figure 20) were detected at all stations during the open-water season in 2022 and 2023 (Figure 21).

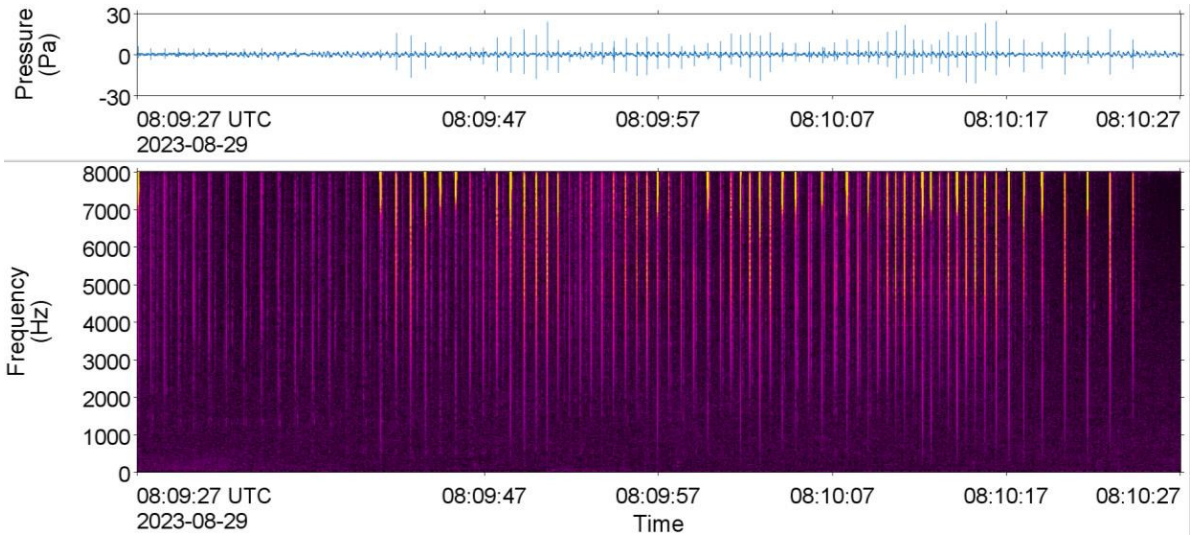

Figure 20. Sperm whale: Spectrogram of clicks recorded at AAR2 on 29 Aug 2023 (2 Hz discrete Fourier Transform (DFT) frequency step, 0.125 s DFT temporal observation window (TOW), 0.03125 s DFT time advance, and Hann window). The spectrogram is 1 min long.

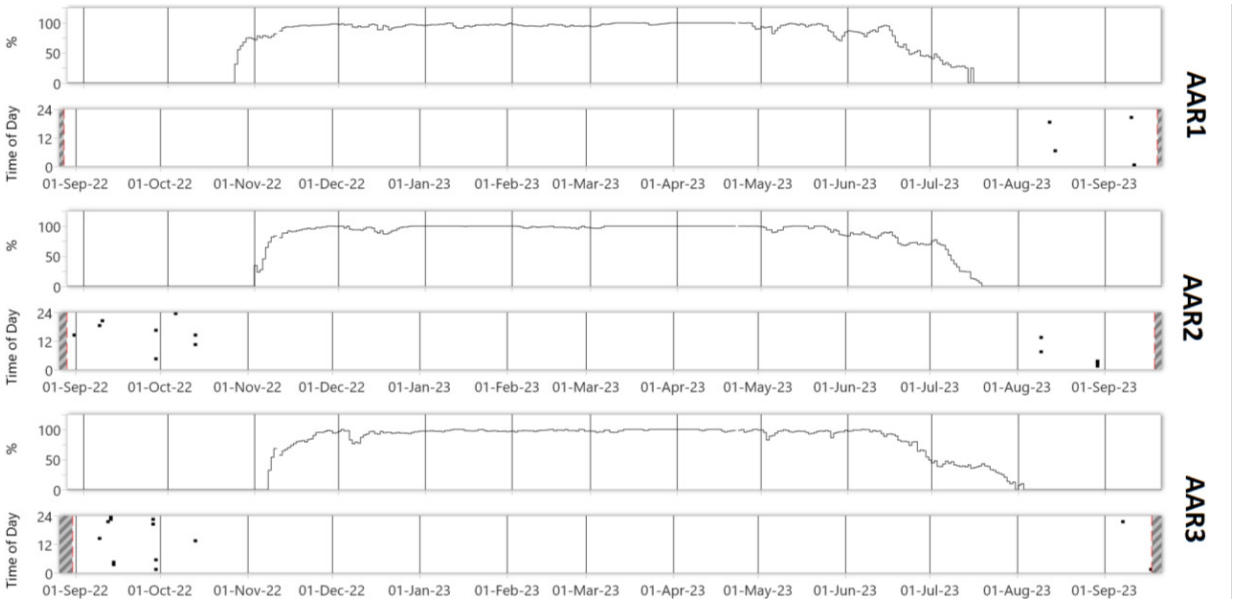

Figure 21. Sperm whale: Daily time series of sea ice concentration (%; top panel) and hourly presence of manual detections (bottom panel) at each monitoring location (AAR1, AAR2, and AAR3) between 28 Aug 2022 and 19 Sep 2023. Sea ice concentration data from EUMETSAT Ocean and Sea Ice Satellite Application Facility, Global sea ice concentration climate data record 1979-2015 (v2.0, 2017), OSI-450, doi: 10.15770/EUM_SAF_OSI_0008, accessed 6 March 2024.

3.3.7. Narwhal

Narwhal vocalizations (including echolocations clicks, buzzes and knocks) (Figure 22) were detected at all stations. Detections were almost exclusively restricted to the periods characterized by sea ice cover. However, while narwhals were only present around ice formation and break up at AAR1, they persisted throughout the ice-covered periods farther south, particularly at AAR3 (Figure 23).

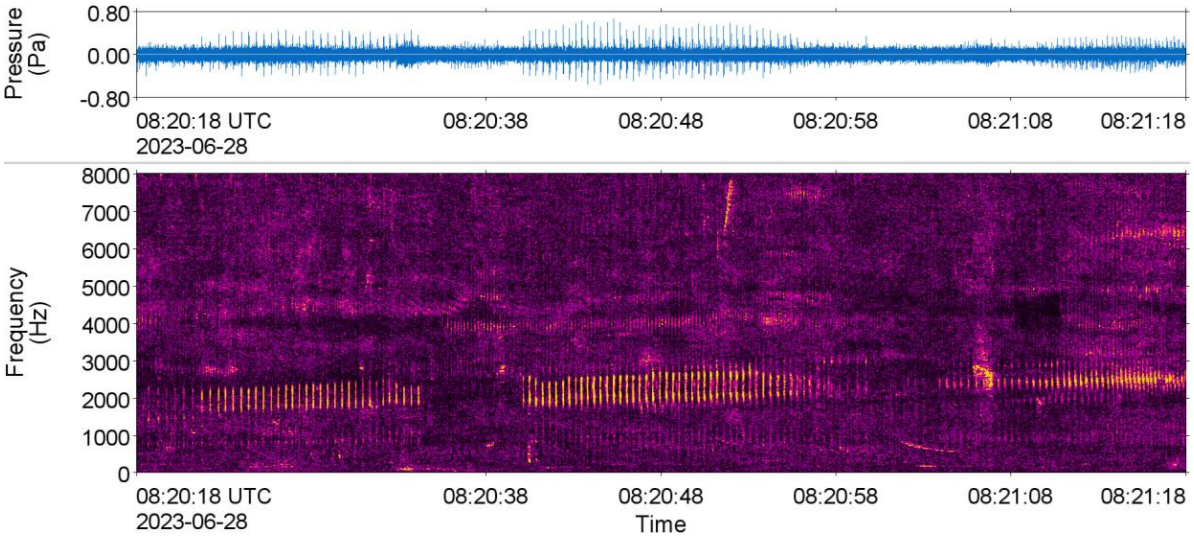

Figure 22. Narwhal: Spectrogram of knocks recorded at AAR1 on 28 Jun 2023 (2 Hz discrete Fourier Transform (DFT) frequency step, 0.125 s DFT temporal observation window (TOW), 0.03125 s DFT time advance, and Hann window). The spectrogram is 1 min long.

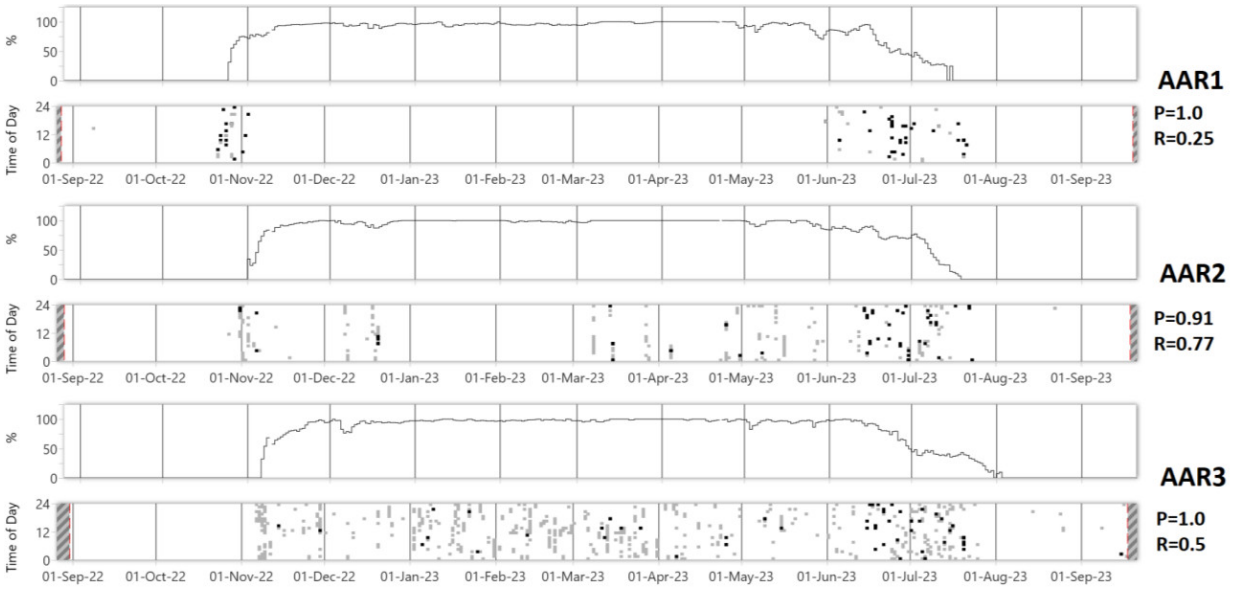

Figure 23. Narwhal: Daily time series of sea ice concentration (%; top panel) and hourly presence of manual (black squares) and automated (grey squares) detections (bottom panel) at each monitoring location (AAR1, AAR2, and AAR3) between 28 Aug 2022 and 19 Sep 2023. Manual detections include both click and non-click (e.g., knocks, buzzes) vocalizations. The automated detections are for the click detector. Sea ice concentration data from EUMETSAT Ocean and Sea Ice Satellite Application Facility, Global sea ice concentration climate data record 1979-2015 (v2.0, 2017), OSI-450, doi: 10.15770/EUM_SAF_OSI_0008, accessed 6 March 2024.

3.3.8. Bearded Seal

Bearded seal trills (Figure 24) were detected manually at all stations with most detections occurring during the second half of June (Figure 25).

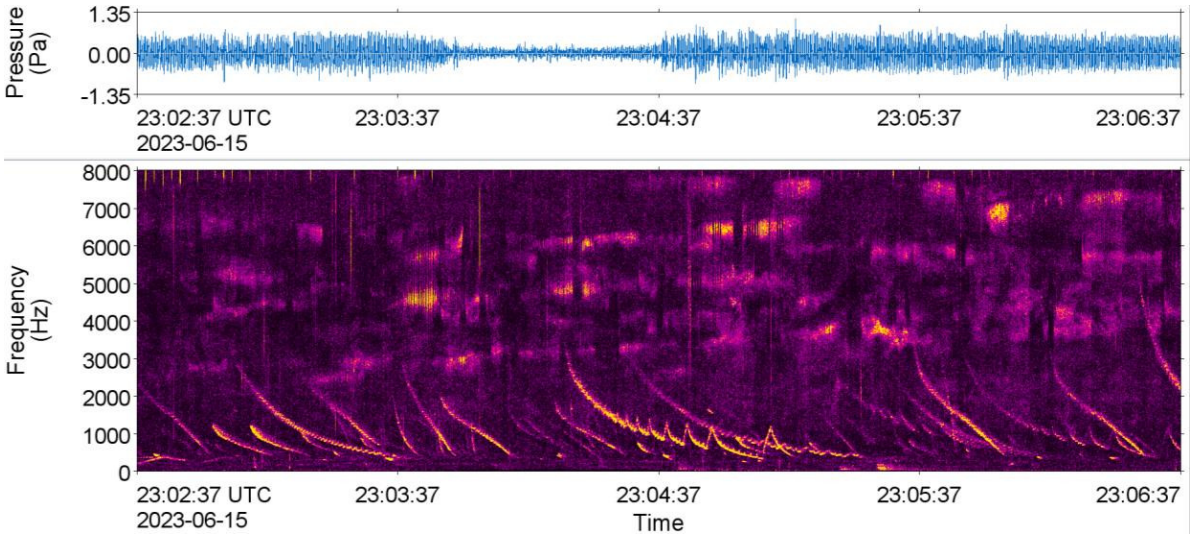

Figure 24. Bearded seal: Spectrogram of trills recorded at AAR2 on 15 Jun 2023 (2 Hz discrete Fourier Transform (DFT) frequency step, 0.125 s DFT temporal observation window (TOW), 0.03125 s DFT time advance, and Hann window). The spectrogram is 4 min long.

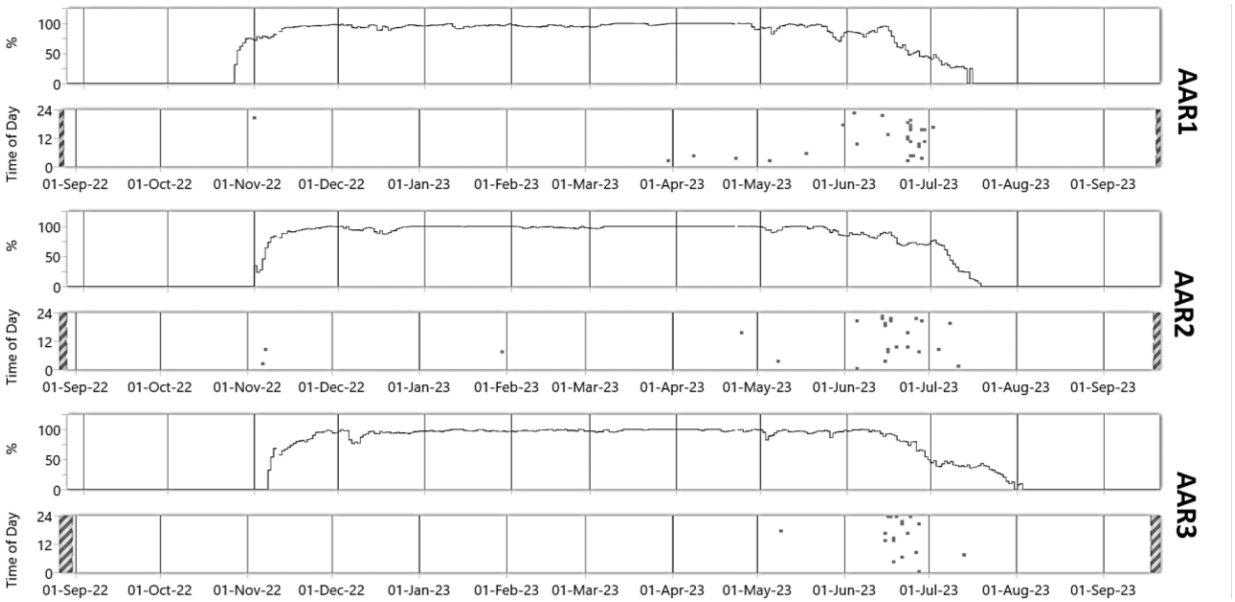

Figure 25. Bearded seal: Daily time series of sea ice concentration (%; top panel) and hourly presence of manual trill detections (bottom panel) at each monitoring location (AAR1, AAR2, and AAR3) between 28 Aug 2022 and 19 Sep 2023. Sea ice concentration data from EUMETSAT Ocean and Sea Ice Satellite Application Facility, Global sea ice concentration climate data record 1979-2015 (v2.0, 2017), OSI-450, doi: 10.15770/EUM_SAF_OSI_0008, accessed 6 March 2024.

3.3.9. Harp Seal

Harp seal vocalizations (Figure 26) were detected manually at AAR1. Although possibly underestimated because based on a limited sample of files manually reviewed, detections were restricted to the periods associated with ice formation and break up (Figure 27).

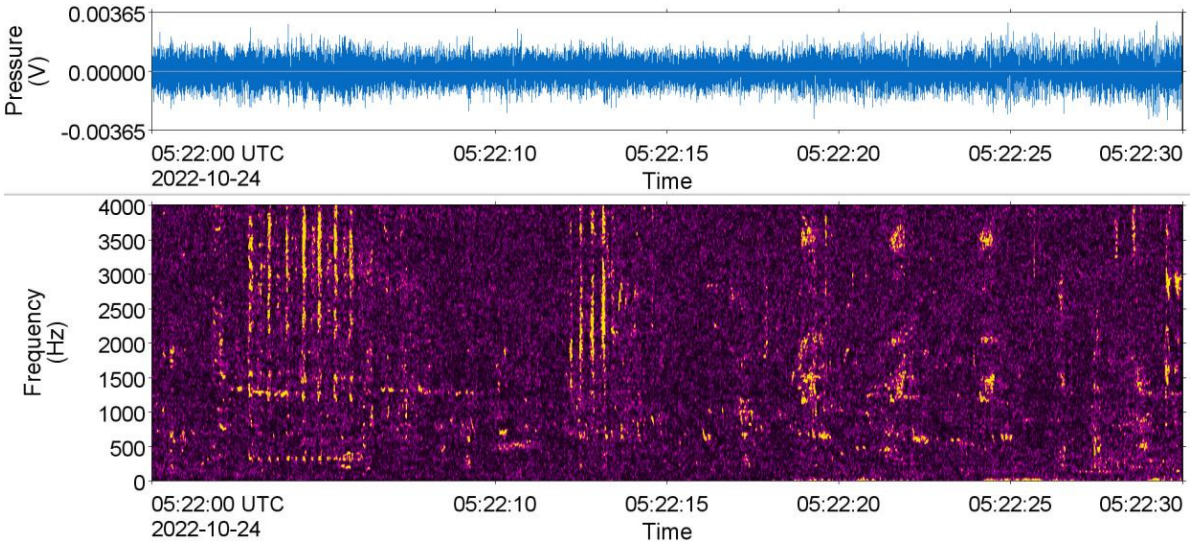

Figure 26. Harp seal: Spectrogram of vocalizations recorded at AAR1 on 24 Oct 2022 (2 Hz discrete Fourier Transform (DFT) frequency step, 0.125 s DFT temporal observation window (TOW), 0.03125 s DFT time advance, and Hann window). The spectrogram is 30 s long.

Figure 27. Harp seal: Daily time series of sea ice concentration (%; top panel) and hourly presence of manual detections (bottom panel) at monitoring location AAR1 between 28 Aug 2022 and 19 Sep 2023. Sea ice concentration data from EUMETSAT Ocean and Sea Ice Satellite Application Facility, Global sea ice concentration climate data record 1979-2015 (v2.0, 2017), OSI-450, doi: 10.15770/EUM_SAF_OSI_0008, accessed 6 March 2024.

4. Conclusions and Recommendations

4.1. Ambient Sound Levels

The nature of the ice along the western side of Baffin Bay were significantly different than what was encountered higher into the arctic as part of the CAUSE and CAATEX experiments. This was particularly notable for the relatively long ice-formation and break up periods (i.e. the ice-concentrations in the mammal figures such as Figure 27).

The collected data were of good quality and appropriate for ambient sound analysis. The ambient sound levels measured here were within the bounds of previous measurements, both for the ice-covered and ice-free seasons. A more detailed analysis comparison of the ambient sound levels during the ice-free, ice-covered, and shoulder periods is recommended. This would then allow for further development and testing of that the under-ice noise model developed previously (Martin et al. 2022, Robinson et al. 2022) using the Baffin Bay data. Such an assessment would also allow for an evaluation of the use of the Regional Ice-Ocean Predictions System (RIOPS) rather than the Global Ice-Ocean Prediction System (GIOPS) as a data source for the model.

As noted in Section 4.3, the acoustic recordings were directional. An investigation of the directional ambient soundscape, particularly during ice formation and break-up, is recommended. This would provide insight into directionality of ice noise that could inform detection of under-ice sound sources.

The variation in yaw (rotation) of AAR2 and AAR3 was less than expected, and much less than was encountered with the CAUSE ‘star’ array mooring, which indicates a stable mooring design. There was evidence of some movement noise in the data from AAR2 and AAR3 which could be reduced by incorporating DRDC’s vibration isolations sections into the mooring above and below the hydrophone array and adding hairy fairing rope (Figure 28) to the section of mooring between the vibration isolation sections.

Figure 28. Section of hairy-fairing rope.

4.2. Marine Mammals

This data set provided a long-term look at areas of the Canadian Arctic that have received little (if any) acoustic monitoring effort before. It confirmed presence of marine mammal species expected in this region. The presence of killer whales in the Canadian Arctic (Higdon et al. 2012, Lefort et al. 2020) was confirmed by these data although a more systematic analysis is needed to better characterize the presence of this species near the recording sites. A closer look at call diversity in relation to those recorded in Canadian waters farther south may offer insights into the range and population structure of northwest Atlantic killer whales. The range of northern bottlenose whales described here (up to AAR2) matches that described based on visual sightings by Feyrer et al. (2024) but provides better documentation of their temporal usage of what appears to be the northern limit of their range. The detections of fin whales at AAR1, albeit likely from distant animals, most likely constitutes the northernmost record of this species in the Atlantic sector of the Arctic.

Because of the value of this dataset for addressing data gaps regarding the year-round occurrence of marine mammals in western Baffin Bay, we recommend performing additional analysis such that the limitations of the manual review protocol applied here (see section 3.3) be addressed and the occurrence of all species be fully characterize using automated detectors. Establishing a long-term monitoring acoustic program in Baffin Bay would be valuable given the expected shifts in species distribution as a result of climate change.

4.3. Vessel Detections

Regular vessel detections occurred during the ice-free season, as well as occasionally during the ice-covered period. A detailed analysis of both types of detections is recommended. The vessel detections were performed using the detector that counts tonals and detects a maximum in the total sound levels (see Section 2.2.2). JASCO has developed a DEMON detector that became available after this data was analyzed; this detector should be applied to the current data set to determine if it improves false alarm rejection during the ice-covered period. A detailed analysis of the remaining under-ice detections should be performed to understand why they are being triggered so that the detector can be improved. The algorithm proposed for long term under-ice surveillance (Kessel et al. 2023) should also be applied to this data to verify its performance. For the ice-free period, we recommend a detailed analysis of the vessel detections, potentially using neural networks, to classify the types of vessels that are using western Baffin Bay.

4.4. Directional Recordings

All three recorders were equipped with directional arrays, which allows the direction of arrival of sounds up to 1 kHz to be estimated. While these analyses were beyond the scope of this report, their application to track the distribution and movement of animals around recorders and assess their densities are promising. Figure 29 illustrates the potential of directional analysis by showing multiple bearded seal and bowhead whales vocalizing under ice in May 2023 at AAR3.

Under an IDEaS project, JASCO is developing methods for determining the range to marine mammals based on modal dispersion and multi-path propagation effects. That project has also developed techniques for counting the minimum number of vocalizing animals and then tracking their locations using target-motion-analysis approaches using directional detections. The project is sponsored by the Department of National Defence to enable better detection, classification and localization of marine

mammals to help mitigate the possible impacts of active sonar exercises on mammals. It is recommended that these techniques be evaluated against the current data.

At the time of finalization of this report, we had not received the vessel tracks required to ground truth the orientation of the arrays and therefore ensure the validity of the bearings. This will be performed as soon as the required data are received such that directional analyses can proceed upon request.

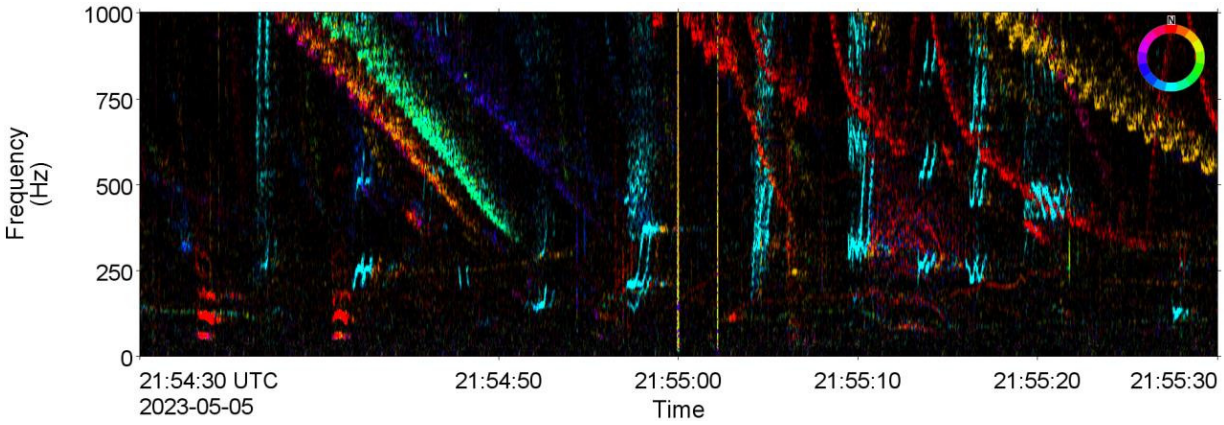

Figure 29. Directogram showing the direction of arrivals of sounds produced by bearded seals and bowhead whales recorded at AAR3 on 5 May 2023. The direction of arrival of the sounds is shown by the colour wheel at the top right of the figure. At least 5 seals and two bowheads were present in this one-minute sample. The bowhead calls from the south (cyan) are showing significant multi-path propagation delays that could be analyzed to determine the range to the calling animal.

Acknowledgements

We thank Emily Maxner and Carmen Lawrence of JASCO for their contribution to the analysis of these data.

Literature Cited

[ANSI] American National Standards Institute and [ASA] Acoustical Society of America. S1.1-2013. *American National Standard: Acoustical Terminology*. NY, USA. https://webstore.ansi.org/Standards/ASA/ANSIASAS12013.

[ISO] International Organization for Standardization. 2017a. *ISO 18405:2017. Underwater acoustics – Terminology*. Geneva. https://www.iso.org/standard/62406.html.

[ISO] International Organization for Standardization. 2017b. *ISO 18406:2017(E). Underwater acoustics – Measurement of radiated underwater sound from percussive pile driving*. Geneva. https://www.iso.org/obp/ui/#iso:std:iso:18406:ed-1:v1:en.

[NRC] National Research Council (US). 2003. *Ocean Noise and Marine Mammals*. National Research Council (US), Ocean Studies Board, Committee on Potential Impacts of Ambient Noise in the Ocean on Marine Mammals. The National Academies Press, Washington, DC, USA. https://doi.org/10.17226/10564.

Ainslie, M.A., J.L. Miksis-Olds, S.B. Martin, K.D. Heaney, C.A.F. de Jong, A.M. von Benda-Beckmann, and A.P. Lyons. 2018. *ADEON Underwater Soundscape and Modeling Metadata Standard*. Version 1.0. Technical report by JASCO Applied Sciences for ADEON Prime Contract No. M16PC00003. 35 p. https://doi.org/10.6084/m9.figshare.6792359.v2.

Amorim, M.C.P. 2006. Diversity of sound production in fish. *In* Ladich, F., S.P. Collin, P. Moller, and B.G. Kapoor (eds.). *Communication in fishes*. Volume 1. Science Publishers. pp. 71-104.

Andrew, R.K., B.M. Howe, and J.A. Mercer. 2011. Long-time trends in ship traffic noise for four sites off the North American West Coast. *Journal of the Acoustical Society of America* 129(2): 642-651. https://doi.org/10.1121/1.3518770.

Au, W.W.L., R.A. Kastelein, T. Rippe, and N.M. Schooneman. 1999. Transmission beam pattern and echolocation signals of a harbor porpoise (*Phocoena phocoena*). *Journal of the Acoustical Society of America* 106(6): 3699-3705. https://doi.org/10.1121/1.428221.

Bailey, H., G. Clay, E.A. Coates, D. Lusseau, B. Senior, and P.M. Thompson. 2010. Using T-PODs to assess variations in the occurrence of coastal bottlenose dolphins and harbour porpoises. *Aquatic Conservation: Marine and Freshwater Ecosystems* 20(2): 150-158. https://doi.org/10.1002/aqc.1060.

Berchok, C.L., D.L. Bradley, and T.B. Gabrielson. 2006. St. Lawrence blue whale vocalizations revisited: Characterization of calls detected from 1998 to 2001. *Journal of the Acoustical Society of America* 120(4): 2340-2354. https://doi.org/10.1121/1.2335676.

Bom, N. 1969. Effect of rain on underwater noise level. *Journal of the Acoustical Society of America* 45(1): 150-156. https://doi.org/10.1121/1.1911351.

Clark, C.W. and J.H. Johnson. 1984. The sounds of the bowhead whale, *Balaena mysticetus*, during the spring migrations of 1979 and 1980. *Canadian Journal of Zoology* 62(7): 1436-1441. https://doi.org/10.1139/z84-206.

Clark, C.W. 1990. Acoustic behaviour of mysticete whales. *In* Thomas, J.A. and R.A. Kastelein (eds.). *Sensory Abilities of Cetaceans*. Springer, Boston, MA. pp. 571-583. https://doi.org/10.1007/978-1-4899-0858-2_40.

Deecke, V.B., J.K.B. Ford, and P.J.B. Slater. 2005. The vocal behaviour of mammal-eating killer whales: Communicating with costly calls. *Animal Behaviour* 69(2): 395-405. https://doi.org/10.1016/j.anbehav.2004.04.014.

Delarue, J.J.-Y., M. Laurinolli, and S.B. Martin. 2009. Bowhead whale (*Balaena mysticetus*) songs in the Chukchi Sea between October 2007 and May 2008. *Journal of the Acoustical Society of America* 126(6): 3319-3328. https://doi.org/10.1121/1.3257201.

Delarue, J.J.-Y., K.A. Kowarski, E.E. Maxner, J.T. MacDonnell, and S.B. Martin. 2018. *Acoustic Monitoring Along Canada's East Coast: August 2015 to July 2017*. Document Number 01279, Environmental Studies Research Funds Report Number 215, Version 1.0. Technical report by JASCO Applied Sciences for Environmental Studies Research Fund, Dartmouth, NS, Canada. 120 pp + appendices.

Ding, W., B. Würsig, and W. Evans. 1995. Comparisons of whistles among seven odontocete species. *In* Kastelein, R.A., J.A. Thomas, and P.E. Nachtigall (eds.). *Sensory Systems of Aquatic Mammals*. De Spil Publishers, The Netherlands. pp. 299-324.

Edds-Walton, P.L. 1997. Acoustic communication signals of mysticetes whales. *Bioacoustics* 8(1-2): 47-60. https://doi.org/10.1080/09524622.1997.9753353.
Erbe, C., A. Verma, R.D. McCauley, A. Gavrilov, and I. Parnum. 2015. The marine soundscape of the Perth Canyon. *Progress in Oceanography* 137: 38-51. https://doi.org/10.1016/j.pocean.2015.05.015.
Erbs, F., S.H. Elwen, and T. Gridley. 2017. Automatic classification of whistles from coastal dolphins of the southern African subregion. *Journal of the Acoustical Society of America* 141(4): 2489-2500. https://doi.org/10.1121/1.4978000.
Feyrer, L.J., J.E. Stanistreet, C. Gomez, M. Adams, J.W. Lawson, S.H. Ferguson, S.G. Heaslip, K.J. Lefort, E. Davidson, et al. 2024. Identifying important habitat for northern bottlenose and Sowerby's beaked whales in the western North Atlantic. *Aquatic Conservation: Marine and Freshwater Ecosystems* 34(1): e4064. https://doi.org/10.1002/aqc.4064.
Ford, J.K.B. and H.D. Fisher. 1978. Underwater acoustic signals of the narwhal (*Monodon monoceros*). *Canadian Journal of Zoology* 56(4): 552-560. https://doi.org/10.1139/z78-079.
Ford, J.K.B. 1989. Acoustic behaviour of resident killer whales (*Orcinus orca*) off Vancouver Island, British Columbia. *Canadian Journal of Zoology* 67(3): 727-745. https://doi.org/10.1139/z89-105.
Gannier, A., S. Fuchs, P. Quèbre, and J.N. Oswald. 2010. Performance of a contour-based classification method for whistles of Mediterranean delphinids. *Applied Acoustics* 71(11): 1063-1069. https://doi.org/10.1016/j.apacoust.2010.05.019.
Garland, E.C., M. Castellote, and C.L. Berchok. 2015. Beluga whale (*Delphinapterus leucas*) vocalizations and call classification from the eastern Beaufort Sea population. *Journal of the Acoustical Society of America* 137(6): 3054-3067. https://doi.org/10.1121/1.4919338.
Hawkins, A.D., L. Casaretto, M. Picciulin, and K. Olsen. 2002. Locating Spawning Haddock by Means of Sound. *Bioacoustics* 12(2-3): 284-286. https://doi.org/10.1080/09524622.2002.9753723.
Heindsmann, T.E., R.H. Smith, and A.D. Arneson. 1955. Effect of rain upon underwater noise levels [Letter to the editor]. *Journal of the Acoustical Society of America* 27(2): 378-379. https://doi.org/10.1121/1.1907897.
Higdon, J.W., D.D.W. Hauser, and S.H. Ferguson. 2012. Killer whales (Orcinus orca) in the Canadian Arctic: Distribution, prey items, group sizes, and seasonality. *Marine Mammal Science* 28(2): E93-E109. https://doi.org/10.1111/j.1748-7692.2011.00489.x.
Hodge, K.B., C.A. Muirhead, J.L. Morano, C.W. Clark, and A.N. Rice. 2015. North Atlantic right whale occurrence near wind energy areas along the mid-Atlantic US coast: Implications for management. *Endangered Species Research* 28(3): 225-234. https://doi.org/10.3354/esr00683.
Jones, J., E. Roth, M. Mahoney, C. Zeller, C. Jackson, K. Kitka, I. Sia, S.M. Wiggins, J.A. Hildebrand, et al. 2011. Seasonal presence of ringed (*Pusa hispida*), ribbon (*Histrophoca fasciata*), and bearded seal (*Erignathus barbatus*) vocalizations in the Chukchi Sea, north of Barrow, Alaska. *Alaska Marine Science Symposium*. Anchorage, AK, USA.
Karlsen, J., A. Bisther, C. Lydersen, T. Haug, and K.M. Kovacs. 2002. Summer vocalisations of adult male white whales (*Delphinapterus leucas*) in Svalbard, Norway. *Polar Biology* 25(11): 808-817. https://doi.org/10.1007/s00300-002-0415-6.
Kessel, R., S.B. Martin, and T.J. Deveau. 2023. *TA-17 High Resolution Arctic Propagation Modelling: Final Report*. Document Number 03024, Version 1.0. Technical report by JASCO Applied Sciences and Seamount Analytics for Atlantic Research Centre, Defence Research and Development Canada.
Knudsen, V.O., R.S. Alford, and J.W. Emling. 1948. Underwater ambient noise. *Journal of Marine Research* 7: 410-429.
Kowarski, K.A., J.J.-Y. Delarue, B.J. Gaudet, and S.B. Martin. 2021. Automatic data selection for validation: A method to determine cetacean occurrence in large acoustic data sets. *JASA Express Letters* 1: 051201. https://doi.org/10.1121/10.0004851.
Krause, B. 2008. Anatomy of the Soundscape: Evolving Perspectives. *Journal of the Audio Engineering Society* 56(1/2): 73-80. http://www.aes.org/e-lib/browse.cfm?elib=14377.
Lefort, K.J., C.J.D. Matthews, J.W. Higdon, S.D. Petersen, K.H. Westdal, C.J. Garroway, and S.H. Ferguson. 2020. A review of Canadian Arctic killer whale (*Orcinus orca*) ecology. *Canadian Journal of Zoology* 98(4): 245-253. https://doi.org/10.1139/cjz-2019-0207.

Martin, S.B., C. Morris, K. Bröker, and C. O'Neill. 2019. Sound exposure level as a metric for analyzing and managing underwater soundscapes. *Journal of the Acoustical Society of America* 146(1): 135-149. https://doi.org/10.1121/1.5113578.

Martin, S.B., B.J. Gaudet, H. Klinck, P.J. Dugan, J.L. Miksis-Olds, D.K. Mellinger, D.A. Mann, O. Boebel, C.C. Wilson, et al. 2021. Hybrid millidecade spectra: A practical format for exchange of long-term ambient sound data. *JASA Express Letters* 1(1). https://doi.org/10.1121/10.0003324.

Martin, S.B., M.M. Zykov, C. Robinson, P.C. Hines, T.J. Deveau, and D.R. Barclay. 2022. *Under-ice Propagation and Ambient Sound Model Improvements: Final Report for W7707/206555 TA-8*. Document Number 02675, Version 1.0. Technical report by JASCO Applied Sciences, Hines Ocean S&T, and 44 N Consulting for Atlantic Research Centre, Defence Research and Development Canada.

Mellinger, D.K. and C.W. Clark. 2003. Blue whale (*Balaenoptera musculus*) sounds from the North Atlantic. *Journal of the Acoustical Society of America* 114(2): 1108-1119. https://doi.org/10.1121/1.1593066.

Menze, S., D.P. Zitterbart, I. van Opzeeland, and O. Boebel. 2017. The influence of sea ice, wind speed and marine mammals on Southern Ocean ambient sound. *Royal Society Open Science* 4(1): 160370. https://doi.org/10.1098/rsos.160370.

Miksis-Olds, J.L. and S.M. Nichols. 2016. Is low frequency ocean sound increasing globally? *Journal of the Acoustical Society of America* 139(1): 501-511. https://doi.org/10.1121/1.4938237.

Møhl, B., M. Wahlberg, P.T. Madsen, L.A. Miller, and A. Surlykke. 2000. Sperm whale clicks: Directionality and source level revisited. *Journal of the Acoustical Society of America* 107(1): 638-648. https://doi.org/10.1121/1.428329.

Mouy, X., M.M. Zykov, and S.B. Martin. 2011. Two-dimensional localization of walruses in shallow water using a ray-tracing model. *Journal of the Acoustical Society of America* 129(4): 2574. https://doi.org/10.1121/1.3588495.

Nieukirk, S.L., K.M. Stafford, D.K. Mellinger, R.P. Dziak, and C.G. Fox. 2004. Low-frequency whale and seismic airgun sounds recorded in the mid-Atlantic Ocean. *Journal of the Acoustical Society of America* 115(4): 1832-1843. https://doi.org/10.1121/1.1675816.

Nordeide, J.T. and E. Kjellsby. 1999. Sound from spawning cod at their spawning grounds. *ICES Journal of Marine Science* 56(3): 326-332. https://doi.org/10.1006/jmsc.1999.0473.

Risch, D., C.W. Clark, P.J. Corkeron, A. Elepfandt, K.M. Kovacs, C. Lydersen, I. Stirling, and S.M. Van Parijs. 2007. Vocalizations of male bearded seals, *Erignathus barbatus*: Classification and geographical variation. *Animal Behaviour* 73(5): 747-762. https://doi.org/10.1016/j.anbehav.2006.06.012.

Risch, D., C.W. Clark, P.J. Dugan, M. Popescu, U. Siebert, and S.M. Van Parijs. 2013. Minke whale acoustic behavior and multi-year seasonal and diel vocalization patterns in Massachusetts Bay, USA. *Marine Ecology Progress Series* 489: 279-295. https://doi.org/10.3354/meps10426.

Robinson, C.L., P.C. Hines, S.B. Martin, and D.R. Barclay. 2022. Spatial, temporal, and spectral variability of ambient noise in the Arctic. *The Journal of the Acoustical Society of America* 151(4_Supplement): A48-A48. https://doi.org/10.1121/10.0010618.

Ross, D. 1976. *Mechanics of Underwater Noise*. Pergamon Press, NY, USA.

Scrimger, J.A., D.J. Evans, G.A. McBean, D.M. Farmer, and B.R. Kerman. 1987. Underwater noise due to rain, hail, and snow. *Journal of the Acoustical Society of America* 81(1): 79-86. https://doi.org/10.1121/1.394936.

Simon, M., K.M. Stafford, K. Beedholm, C.M. Lee, and P.T. Madsen. 2010. Singing behavior of fin whales in the Davis Strait with implications for mating, migration and foraging. *Journal of the Acoustical Society of America* 128(5): 3200-3210. https://doi.org/10.1121/1.3495946.

Širović, A., A. Rice, E. Chou, J.A. Hildebrand, S.M. Wiggins, and M.A. Roch. 2015. Seven years of blue and fin whale call abundance in the Southern California Bight. *Endangered Species Research* 28(1): 61-76. https://doi.org/10.3354/esr00676.

Stafford, K.M., K.L. Laidre, and M.P. Heide-Jørgensen. 2012. First acoustic recordings of narwhals (*Monodon monoceros*) in winter. *Marine Mammal Science* 28(2): E197-E207. https://doi.org/10.1111/j.1748-7692.2011.00500.x.

Stirling, I., W. Calvert, and C. Spencer. 1987. Evidence of stereotyped underwater vocalizations of male Atlantic walruses (*Odobenus rosmarus rosmarus*). *Canadian Journal of Zoology* 65(9): 2311-2321. https://doi.org/10.1139/z87-348.

Strasberg, M. 1979. Nonacoustic noise interference in measurements of infrasonic ambient noise. *Journal of the Acoustical Society of America* 66(5): 1487-1493. https://doi.org/10.1121/1.383543.
Terhune, J.M. 1994. Geographical variation of harp seal underwater vocalizations. *Canadian Journal of Zoology* 72(5): 892-897. https://doi.org/10.1139/z94-121.
Tyack, P.L. and C.W. Clark. 2000. Communication and Acoustic Behavior of Dolphins and Whales. (Chapter 4) *In* Au, W.W.L., R.R. Fay, and A.N. Popper (eds.). *Hearing by Whales and Dolphins*. Springer, New York. pp. 156-224. https://doi.org/10.1007/978-1-4612-1150-1_4.
Urazghildiiev, I.R. and S.M. Van Parijs. 2016. Automatic grunt detector and recognizer for Atlantic cod (*Gadus morhua*). *Journal of the Acoustical Society of America* 139(5): 2532-2540. https://doi.org/10.1121/1.4948569.
Urick, R.J. 1983. *Principles of Underwater Sound*. 3rd edition. McGraw-Hill, New York, London. 423 p.
Walmsley, S.F., L.E. Rendell, N.E. Hussey, and M. Marcoux. 2020. Vocal sequences in narwhals (*Monodon monoceros*). *Journal of the Acoustical Society of America* 147(2): 1078-1091. https://doi.org/10.1121/10.0000671.
Watkins, W.A. 1980. Acoustics and the Behavior of Sperm Whales. *In* Busnel, R.-G. and J.F. Fish (eds.). *Animal Sonar Systems*. Volume 28. Springer, Boston. pp. 283-290. https://doi.org/10.1007/978-1-4684-7254-7_11.
Wenz, G.M. 1962. Acoustic Ambient Noise in the Ocean: Spectra and Sources. *Journal of the Acoustical Society of America* 34(12): 1936-1956. https://doi.org/10.1121/1.1909155.
Willis, J. and F.T. Dietz. 1961. Effect of Tidal Currents on 25 cps Shallow Water Ambient Noise Measurements. *Journal of the Acoustical Society of America* 33(11): 1659-1659. https://doi.org/10.1121/1.1936636.

Appendix A. Acoustic Data Analysis

The sampled data were processed for ambient sound analysis, vessel noise detection, and detection of all marine mammal vocalizations with JASCO's PAMlab acoustic analysis software suite. The major processing stages are outlined in Figure A-1.

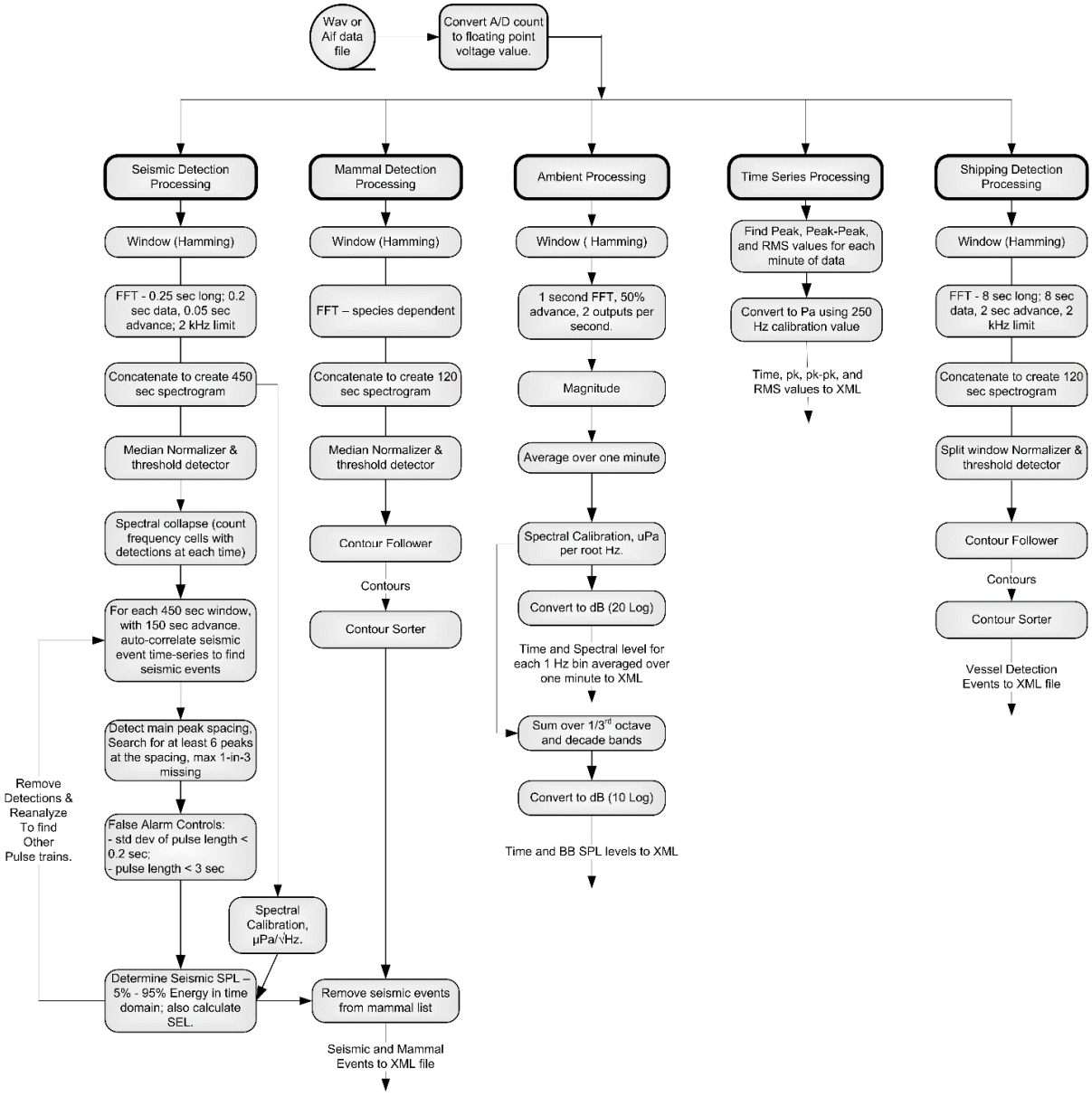

Figure A-1. Major stages of the automated acoustic analysis process performed with JASCO's PAMlab software suite.

A.1. Acoustic Metrics

Underwater sound pressure amplitude is quantified in decibels (dB) relative to a fixed reference pressure of p_0 = 1 µPa. Because the perceived loudness of sound, especially pulsed sound such as from seismic airguns, pile driving, and sonar, is not generally proportional to the instantaneous acoustic pressure, several sound level metrics are commonly used to evaluate sound and its effects on marine life. Here we provide specific definitions of relevant metrics used in the accompanying report. Where possible, we follow International Organization for Standardization definitions and symbols for sound metrics (e.g., ISO 18405:2017a, ANSI S1.1-2013).

The zero-to-peak sound pressure, or peak sound pressure (PK or L_{pk}; dB re 1 µPa), is the decibel level of the maximum instantaneous sound pressure in a stated frequency band attained by an acoustic pressure signal, $p(t)$:

$$L_{\text{pk}} = 10 \log_{10} \frac{p_{\text{pk}}^2}{p_0^2} = 20 \log_{10} \frac{p_{\text{pk}}}{p_0} = 20 \log_{10} \frac{\max|p(t)|}{p_0} \tag{A-1}$$

PK is often included as a criterion for assessing whether a sound is potentially injurious; however, because it does not account for the duration of an acoustic event, it is generally a poor indicator of perceived loudness.

The sound pressure level (SPL or L_p; dB re 1 µPa) is the root-mean-square (rms) pressure level in a stated frequency band over a specified time window (T; s):

$$L_p = 10 \log_{10} \frac{p_{\text{rms}}^2}{p_0^2} = 10 \log_{10} \left(\frac{1}{T} \int_T p^2(t)\, dt \Big/ p_0^2 \right) \tag{A-2}$$

It is important to note that SPL always refers to an rms pressure level (i.e., a quadratic mean over a time interval) and therefore not instantaneous pressure at a fixed point in time. The SPL can also be defined as the *mean-square* pressure level, given in decibels relative to a reference value of 1 µPa^2 (i.e., in dB re 1 µPa^2). The two definitions of SPL are numerically equivalent, differing only in reference value.

The SPL can also be calculated using a time weighting function, $g(t)$:

$$L_p = 10 \log_{10} \left(\frac{1}{T} \int_T g(t)\, p^2(t)\, dt \Big/ p_0^2 \right) \text{ dB} \tag{A-3}$$

In many cases, the start time of the integration is marched forward in small time steps to produce a time-varying SPL function. For short acoustic events, such as sonar pulses and marine mammal vocalizations, it is important to choose an appropriate time window that matches the duration of the signal. For in-air studies, when evaluating the perceived loudness of sounds with rapid amplitude variations in time, the time weighting function $g(t)$ is often set to a decaying exponential function that emphasizes more recent pressure signals. This function mimics the leaky integration nature of mammalian hearing. For example, human-based fast time-weighted SPL ($L_{p,\text{fast}}$) applies an exponential function with time constant 125 ms. A related simpler approach used in underwater acoustics sets $g(t)$ to a boxcar (unity amplitude) function of width 125 ms; the results can be referred to as $L_{p,\text{boxcar 125ms}}$.

Another approach, historically used to evaluate SPL of impulsive signals underwater (e.g., from pile driving or seismic airguns), defines $g(t)$ as a boxcar function with edges set to the times corresponding to 5 and 95 % of the cumulative square pressure function encompassing the duration of an impulsive

acoustic event. This calculation is applied individually to each impulse signal, and the results have been referred to as 90 % SPL ($L_{p,90}$).

The sound exposure level (SEL or L_E; dB re 1 µPa^2 s) is the time-integral of the squared acoustic pressure over a duration (T):

$$L_E = 10 \log_{10} \left(\int_T p^2(t)\, dt \Big/ T_0 p_0^2 \right) \text{ dB} \tag{A-4}$$

where T_0 is a reference time interval of 1 s. SEL continues to increase with time when non-zero pressure signals are present. It is a dose-type measurement, so the integration time applied must be carefully considered for its relevance to impact to the exposed recipients. SEL can be calculated over a fixed duration, such as the time of a single event or a period with multiple acoustic events.

When applied to pulsed sounds, SEL can be calculated by summing the SEL of the N individual pulses. For a fixed duration, the square pressure is integrated over the duration of interest. For multiple events, the SEL can be computed by summing (in linear units) the SEL of the N individual events:

$$L_{E,N} = 10 \log_{10} \left(\sum_{i=1}^{N} 10^{\frac{L_{E,i}}{10}} \right) \tag{A-5}$$

Because the SPL and SEL are both computed from the integral of square pressure, these metrics are related numerically by the following expression, which depends only on the duration of the time window T:

$$L_p = L_E - 10 \log_{10}(T) \tag{A-6}$$

Likewise, the SPL(T_{90}) and SEL metrics are related by:

$$L_{p,90} = L_E - 10 \log_{10}(T_{90}) - 0.458 \tag{A-7}$$

where the 0.458 dB factor accounts for the 10 % of pulse SEL missing from the SPL(T_{90}) integration time window.

Energy equivalent SPL (L_{eq}; dB re 1 µPa) denotes the SPL of a stationary (constant amplitude) sound that generates the same SEL as the signal being examined, $p(t)$, over the same time period, T:

$$L_{\text{eq}} = 10 \log_{10} \left(\frac{1}{T} \int_T p^2(t)\, dt \Big/ p_0^2 \right) \tag{A-8}$$

The equations for SPL and the energy-equivalent SPL are numerically identical. Conceptually, the difference between the two metrics is that the SPL is typically computed over short periods (typically of 1 s or less) and tracks the fluctuations of a non-steady acoustic signal, whereas the L_{eq} reflects the average SPL of an acoustic signal over time periods typically of 1 min to several hours.

A.2. Decidecade Band Analysis

The distribution of a sound's power with frequency is described by the sound's spectrum. The sound spectrum can be split into a series of adjacent frequency bands. Splitting a spectrum into 1 Hz wide bands, called passbands, yields the power spectral density of the sound. These values directly compare to the Wenz curves, which represent typical deep ocean sound levels (see Figure 2) (Wenz 1962). This splitting of the spectrum into passbands of a constant width of 1 Hz, however, does not represent how animals perceive sound.

Animals perceive exponential increases in frequency rather than linear increases, so analyzing a sound spectrum with passbands that increase exponentially in size better approximates real-world scenarios. In underwater acoustics, a spectrum is commonly split into decidecade bands, which are one tenth of a decade wide. A decidecade is sometimes referred to as a "1/3-octave" because one tenth of a decade is approximately equal to one third of an octave. Each decade represents a factor of 10 in sound frequency. Each octave represents a factor of 2 in sound frequency. The centre frequency of the ith decidecade band, $f_c(i)$, is defined as:

$$f_c(i) = 10^{\frac{i}{10}} \text{ kHz} \tag{A-9}$$

and the low (f_{lo}) and high (f_{hi}) frequency limits of the ith decidecade band are defined as:

$$f_{\text{lo},i} = 10^{\frac{-1}{20}} f_c(i) \text{ and } f_{\text{hi},i} = 10^{\frac{1}{20}} f_c(i) \tag{A-10}$$

The decidecade bands become wider with increasing frequency, and on a logarithmic scale the bands appear equally spaced (Figure A-2).

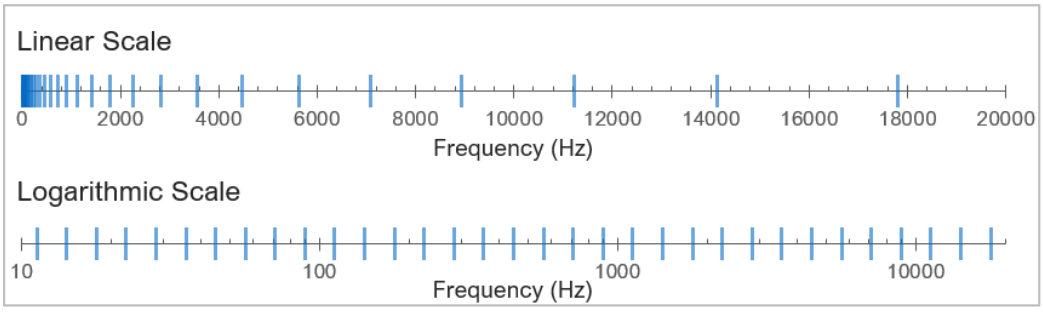

Figure A-2. Decidecade frequency bands (vertical lines) shown on (top) a linear frequency scale and (bottom) a logarithmic scale. On the logarithmic scale, the bands are equally spaced.

The sound pressure level in the ith band ($L_{p,i}$) is computed from the spectrum $S(f)$ between $f_{lo,i}$ and $f_{hi,i}$:

$$L_{p,i} = 10 \log_{10} \int_{f_{\text{lo},i}}^{f_{\text{hi},i}} S(f)\, \mathrm{d}f \text{ dB}\,. \tag{A-11}$$

Summing the sound pressure level of all the bands yields the broadband sound pressure level:

$$\text{Broadband SPL} = 10 \log_{10} \sum_i 10^{\frac{L_{p,i}}{10}} \text{ dB}\,. \tag{A-12}$$

Figure A-3 shows an example of how the decidecade band sound pressure levels compare to the sound pressure spectral density levels of an ambient sound signal. Because the decidecade bands are wider than 1 Hz, the decidecade band SPL is higher than the spectral levels at higher frequencies. Decidecade band analysis can be applied to continuous and impulsive sound sources. For impulsive sources, the decidecade band SEL is typically reported.

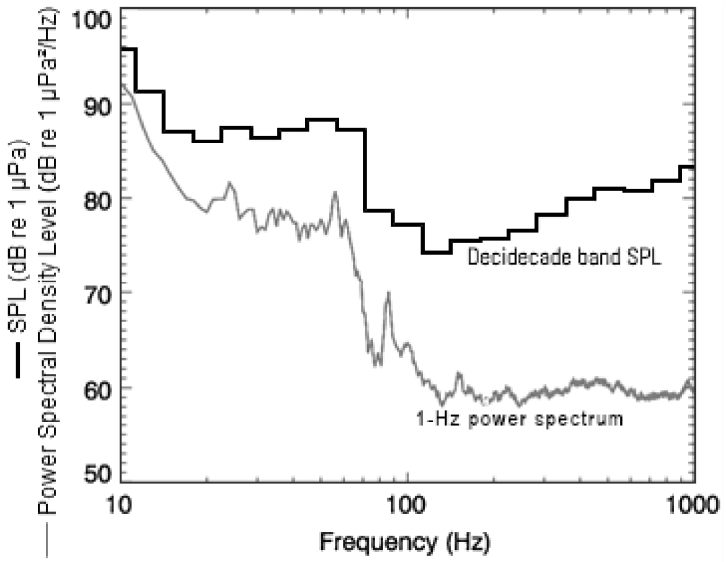

Figure A-3. Sound pressure spectral density levels and the corresponding decidecade band sound pressure levels (SPL) of example ambient sound shown on a logarithmic frequency scale. Because the decidecade bands are wider with increasing frequency, the decidecade band SPL is higher than the power spectrum, which is based on bands with a constant width of 1 Hz.

Table A-1. Decidecade band centre and limiting frequencies (Hz).

Band	Lower frequency	Nominal centre frequency	Upper frequency	Band	Lower frequency	Nominal centre frequency	Upper frequency
10	8.9	10.0	11.2	33	1778	1995	2239
11	11.2	12.6	14.1	34	2239	2512	2818
12	14.1	15.8	17.8	35	2818	3162	3548
13	17.8	20.0	22.4	36	3548	3981	4467
14	22.4	25.1	28.2	37	4467	5012	5623
15	28.2	31.6	35.5	38	5623	6310	7079
16	35.5	39.8	44.7	39	7079	7943	8913
17	44.7	50.1	56.2	40	8913	10000	11220
18	56.2	63.1	70.8	41	11220	12589	14125
19	70.8	79.4	89.1	42	14260	16000	17952
20	89.1	100.0	112.2	43	17825	20000	22440
21	112	126	141	44	22281	25000	28050
22	141	158	178	45	28074	31500	35344
23	178	200	224	46	35650	40000	44881
24	224	251	282	47	44563	50000	56101
25	282	316	355	48	56149	63000	70687
26	355	398	447	49	71300	80000	89761
27	447	501	562	50	89125	100000	112202
28	562	631	708	51	111406	125000	Above Nyquist
29	708	794	891				

Table A-2. Decade band centre and limiting frequencies (Hz).

Decade band	Lower frequency	Nominal centre frequency	Upper frequency
A	8.9	50	89.1
B	89.1	500	891
C	891	5,000	8913
D	8913	50,000	89125

Appendix B. Marine Mammal Detection Methodology

B.1. Automated Click Detector for Odontocetes

Figure B-1 shows how we apply an automated click detector/classifier to the data to detect clicks from odontocetes. This detector/classifier is based on the zero-crossings in the acoustic time series. Zero-crossings are the rapid oscillations of a click's pressure waveform above and below the signal's normal level. Clicks are detected by the following steps:

1. The raw data are high-pass filtered to remove all energy below 5 kHz. This removes most energy from sources other than odontocetes (such as shrimp, vessels, wind, and cetacean tonal calls) yet allows the energy from all marine mammal click types to pass.
2. The filtered samples are summed to create a 0.334 ms rms time series. Most marine mammal clicks have a 0.1–1 ms duration.
3. Possible click events are identified with a split-window normalizer that divides the 'test' bin of the time series by the mean of the 6 'window' bins on either side of the test bin, leaving a 'notch' that is 1-bin wide.
4. A Teager-Kaiser energy detector identifies possible click events.
5. The high-pass filtered data are searched to find the maximum peak signal within 1 ms of the detected peak.
6. The high-pass filtered data are searched backwards and forwards to find the time span when the local data maxima are within 9 dB of the maximum peak. The algorithm allows for two zero-crossings to occur where the local peak is not within 9 dB of the maximum before stopping the search. This defines the time window of the detected click.
7. The classification parameters are extracted. The number of zero crossings within the click, the median time separation between zero crossings, and the slope of the change in time separation between zero-crossings are computed. The slope parameter helps identify beaked whale clicks, because beaked whales can be identified by the increase in frequency (upsweep) of their clicks.
8. The Mahalanobis distance between the extracted classification parameters and the templates of known click types is computed. The covariance matrices for the known click types (computed from thousands of manually identified clicks for each species) are stored in an external file. Each click is classified as a type with the minimum Mahalanobis distance unless none of them are less than the specified distance threshold.

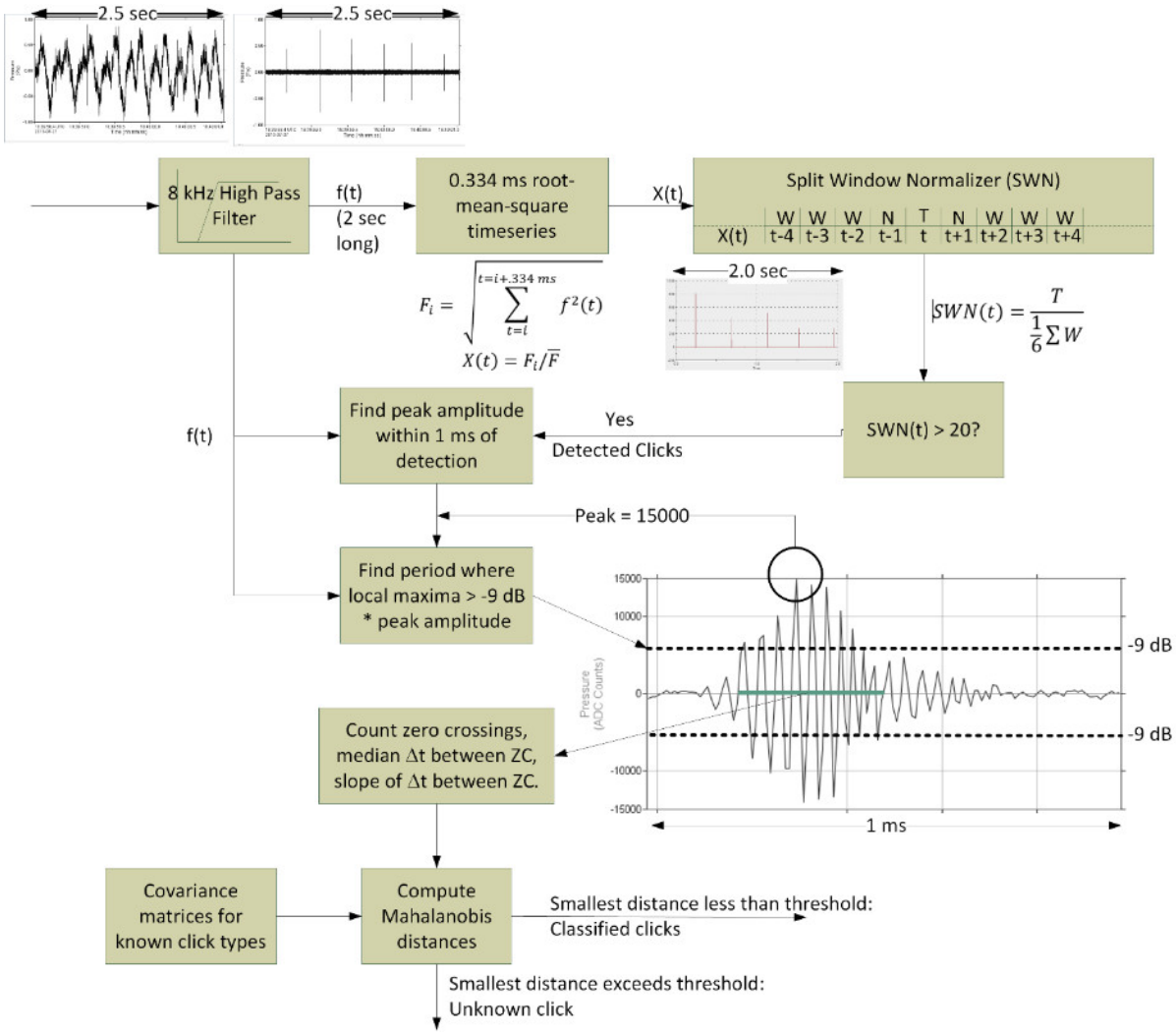

Figure B-1. Flowchart of the automated click detector/classifier process.

Odontocete clicks occur in groups called click trains. Each species has a characteristic inter-click-interval (ICI) and number of clicks per train. The automated click detector includes a second stage that associates individual clicks into trains (Figure B-2). The automated click train detector performs the following steps:

1. Queue clicks for N seconds, where N is twice the maximum number of clicks per train times the maximum ICI.
2. Search for all clicks within the window that have Mahalanobis distances less than 11 for a species of interest (this finds 80 % of all clicks for the species as defined by the template).
3. Create a candidate click train if:
   a. The number of clicks is greater or equal to the minimum number of clicks in a train;
   b. The maximum time between any two clicks is less than 2.5 times the maximum ICI, and
   c. The smallest Mahalanobis distance for all clicks in the candidate train is less than 4.1.
4. Create a new ‘time series’ with a value of 1 at the time of arrival for each click and zero everywhere else (using a ‘time series’ with a bin duration of 0.5 ms).

5. Apply a Hann window to the time series, and then compute the cepstrum.
6. A click train is classified if a peak in the cepstrum with an amplitude greater than five times the standard deviation of the cepstrum occurs at a quefrency between the minimum maximum ICI.
7. For each click related to the previous Ncepstrum, create a new time series and compute ICI. If there is a good match, then extend the click train.
8. Output a species click train detection if the click features, total clicks, and mean ICI match the species.

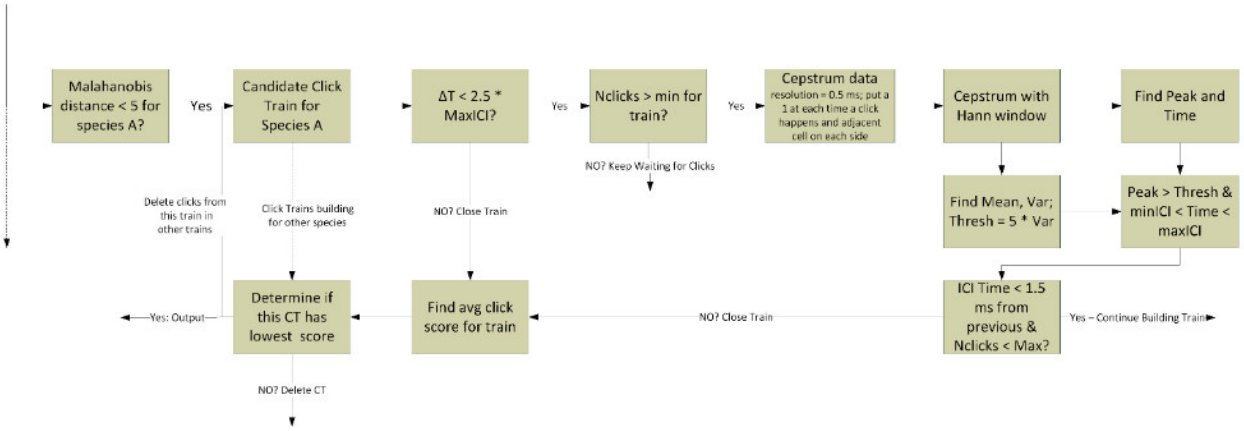

Figure B-2. Flowchart of the click train automated detector/classifier process.

B.2. Automated Tonal Signal Detection

Marine mammal tonal acoustic signals are automatically detected using a contour detection and following algorithm that is depicted in (Figure B-3). The algorithm has the following steps:

1. Create spectrograms of the appropriate resolution for each mammal vocalization type that were normalized by the median value in each frequency bin for each detection window (Table B-1).
2. Join adjacent bins and create contours via a contour-following algorithm (Figure B-4).
3. Apply a sorting algorithm to determine if the contours match the definition of a marine mammal vocalization (Table B-2).

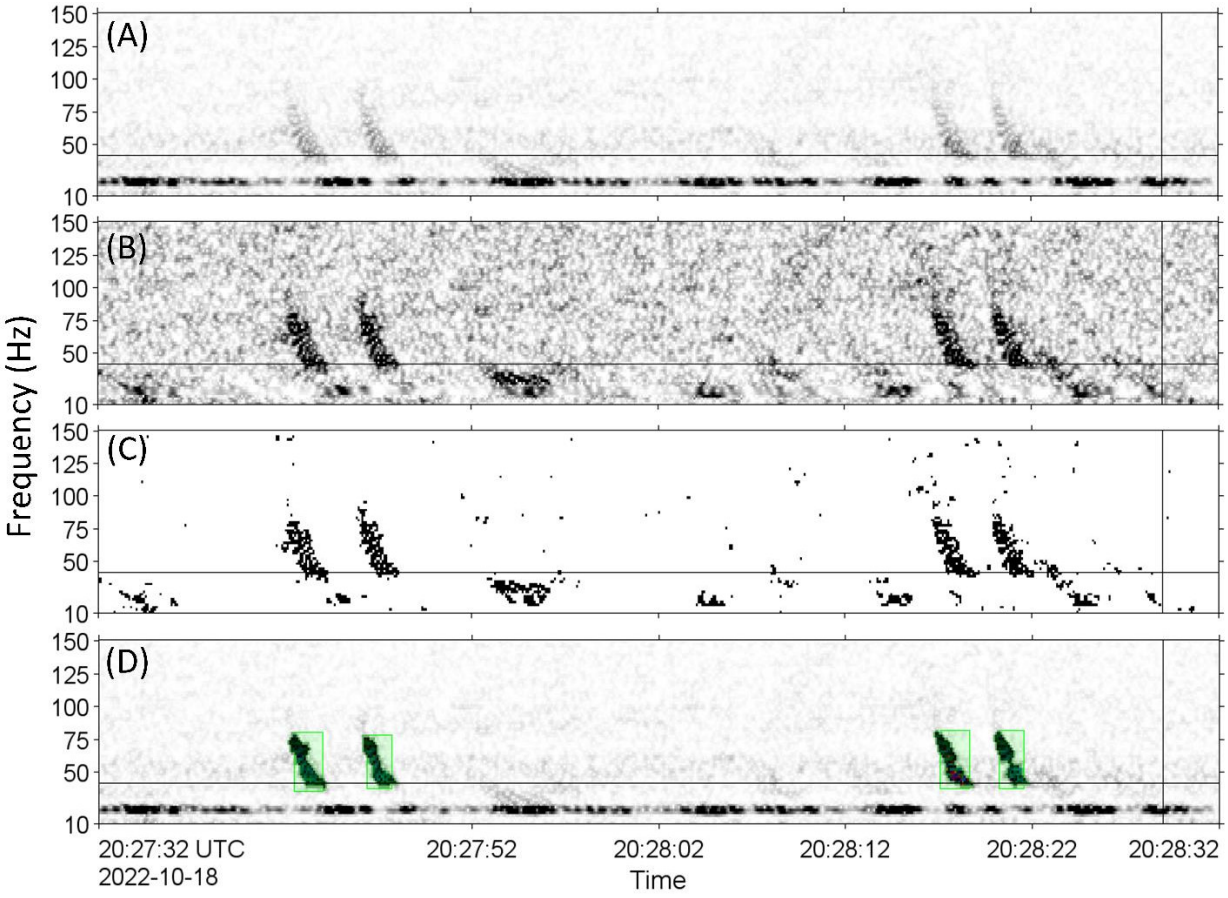

Figure B-3. Illustration of the contour detection process. (A) A spectrogram is generated at the frequency and time resolutions appropriate for the tonal calls of interest. (B) A median normalizer is applied at each frequency. (C) The data is turned into a binary representation by setting all normalized values less than the threshold to 0 and all values greater than the threshold to 1. (D) The regions that are '1' in the binary spectrogram are connected to create contours, which are then sorted to detect signals of interest, shown here as green overlays.

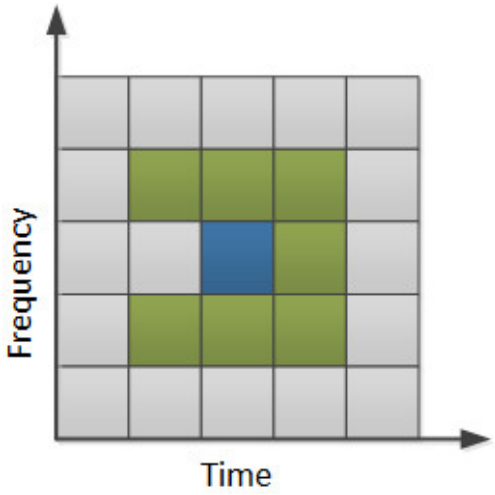

Figure B-4. Illustration of the search area used to connect spectrogram bins. The blue square represents a bin of the binary spectrogram equalling 1 and the green squares represent the potential bins it could be connected to. The algorithm advances from left to right, so grey cells left of the test cell need not be checked.

The tonal signal detector is expanded into a pulse train detector through the following steps:

1. Detect and classify contours as described in Steps 1 and 2 above.
2. A sorting algorithm determines if any series of contours can be assembled into trains that match a pulse train template (Table B-3).

Table B-1. Discrete Fourier Transform (DFT) and detection window settings for all automated contour-based detectors used to detect tonal vocalizations of marine mammal species expected in the data. Values are based on JASCO's experience and empirical evaluation of various data sets. Due to the overlapping characteristics of some species' signals, automated detectors developed for a particular signal (Primary species (signal) targeted), can also effectively detect the signals of other species (Other species (signal) targeted). For some signals, JASCO applies many automated detectors and during manual validation determines which perform best.

Automated detector	Primary species (signal) targeted	Other species (signal) targeted	Discrete Fourier transform			Detection window (s)	Detection threshold
			Frequency step (Hz)	Temporal observation window (s)	Time advance (s)		
LFMoan	Bowhead, humpback whale (moan)	Blue whale (D call), fin whale (40 Hz call)	2	0.25	0.05	10	3
MFMoanLow			4	0.2	0.05	5	3
MFMoanLowHT			4	0.2	0.05	5	5
MFMoanHigh			8	0.125	0.05	5	3
MFMoanHighHT			8	0.125	0.05	5	5
ShortLow		Pinnipeds (moan), fish (grunt)	7	0.17	0.025	10	3
Atl_BW_GL_IM	Blue whale (A-B song)	NA	0.125	2	0.5	40	4
Atl_BlueWhale_IM			0.125	2	0.5	40	4
Atl_BlueWhale_IM_HT			0.125	2	0.5	40	6
Atl_BlueWhale_IM2			0.125	2	0.5	120	4
Atl_BlueWhale_IM2_HT			0.125	2	0.5	120	6
NPac_BW_D	Blue whale (D call)	Sei whale (downsweep)	2	0.25	0.05	10	2
NPac_BW_D_HT			2	0.25	0.05	10	4
Atl_FinWhale_21	Fin whale (20 Hz pulse)	NA	1	0.2	0.05	5	1.7
Atl_FinWhale_21_HT			1	0.2	0.05	5	3.7
Atl_FinWhale_21.2			1	0.2	0.05	5	4
Atl_FinWhale_21.2_HT			1	0.2	0.05	5	6
VLFMoan			2	0.2	0.05	15	4
Atl_FW130	Fin whale (130 Hz call)	Humpback whale (moan), Right whale (moan)	2	0.2	0.05	5	3
Narwhal_LFbuzz	Narwhal (buzz)	Beluga (buzz)	16	0.03	0.015	5	2
Narwhal_HFbuzz			64	0.01	0.005	5	2.5
Narwhal_KnockTrain	Narwhal (knock)	NA	64	0.01	0.005	40	2
Narwhal_Whistle	Narwhal (whistle)	Beluga (whistle)	4	0.05	0.01	5	3.5
Beardedseal_downsweep Beardedseal_upsweep	Bearded seal (trill)	NA	2	0.2	0.05	10	3
Beardedseal_fulltrill			4	0.25	0.125	10	3
Ribbonseal_downsweep	Ribbon seal (downsweep)	Beluga, narwhal (whistle), Bowhead whale (moan)	4	0.1	0.05	5	3
Ringedseal_LFdoublethump	Ringed seal (double thump)	NA	20	0.05	0.025	5	4
Walrus_knock	Walrus (knock)	NA	32	0.03125	0.016	5	4
WhistleHigh_Suppress	Beluga (whistle with energy between 4–20 kHz)	Pilot, killer whale (whistle)	64	0.015	0.005	10	1.5
WhistleHigh_Quiet			64	0.015	0.005	10	1.5
WhistleHigh_Loud			64	0.015	0.005	10	4.5
WhistleLow_Suppress	Pilot, killer whale (whistle with energy between 1–10 kHz)	Small dolphin, narwhal (whistle)	8	0.125	0.05	10	1.5
WhistleLow_Quiet			8	0.125	0.05	10	1.5
WhistleLow_Loud			8	0.125	0.05	10	4.5

Table B-2. A sample of vocalization sorter definitions for the tonal vocalizations of cetacean species expected in the area. Automated detectors are capable of triggering on species and signals beyond those targeted.

Automated detector	Frequency (Hz)	Duration (s)	Bandwidth (Hz)	Other parameters
LFMoan	40–250	0.50–10.00	>15	MIB <50 Hz
MFMoanLow MFMoanLowHT	100–700	0.50–5.00	>50	f_{min} <450 Hz, MIB <200 Hz
MFMoanHigh MFMoanHighHT	500–2500	0.50–5.00	>150	f_{min} <1500 Hz, MIB <300 Hz
Narwhal_LFbuzz	14,000–100,000	0.10–10.00	>3000	None
Narwhal_HFbuzz	1000–10,000	0.50–5.00	>1000	f_{min} <5000 Hz
Narwhal_KnockTrain	1000–8000	0.04–0.005	NA	0.03–0.5 s pulse gap, 0.5–30 s train length
Narwhal_Whistle	1000–20,000	0.50–5.00	20–1000	f_{min} <9000 Hz
Beardedseal_downsweep	200–1500	1.00–10.00	>100	−30<SR<−500 Hz/s
Beardedseal_upsweep	150–2000	1.00–6.00	>100	100<SR<1000 Hz/s
Beardedseal_fulltrill	125–8200	10.00–90.00	>500	−5<SR<−150 Hz/s
Ribbonseal_downsweep	20–2000	0.60–2.50	>400	NA
Ringedseal_LFdoublethump	10–250	0.20–1.00	>20	f_{min} <50 Hz
Walrus_knock	20–8000	0.03–0.30	>1200	f_{min} <750 Hz
ShortLow	30–400	0.08–0.60	>25	None
VLFMoan	10–100	0.30–10.00	>10	f_{min} <40 Hz
WhistleLow_Suppress	1000–10,000	0.80–5.00	>300	f_{min} <5000 Hz, MIB <1000 Hz, Min_BW>50 Hz, suppress detections for SPL >125 dB from 50–1000 Hz
WhistleHigh_Suppress	4000–12,000	0.30–5.00	>700	MIB <2000 Hz, Suppress detections for SPL >125 dB from 50–1000 Hz
WhistleLow_Loud WhistleLow_Quiet	1000–10,000	0.80–5.00	>300	f_{min} 5000 Hz, MIB <1000 Hz, MultiComponent = 1, minComponentduration = 0.4 s, Min_BW>50Hz
WhistleHigh_Loud WhistleHigh_Quiet	4000–20,000	0.30–5.00	>700	MIB <2000 Hz
Alt_Blue_Whale_GL_IM	14–22	8.00–30.00	1-5	f_{min} <18 Hz, 16.5< f_{peak} <17.5Hz, −500SR<SR<0 Hz/s
Atl_BlueWhale_IM Atl_BlueWhale_IM_HT	14–22	8.00–30.00	1–5	f_{min} <18 Hz, 16.5< f_{peak} <18 Hz, −500<SR<0 Hz/s
Atl_BlueWhale_IM2 Atl_BlueWhale_IM2_HT	15–22	8.00–30.00	1–5	f_{min} <18 Hz
NPac_BlueWhale_D NPac_BlueWhale_D_HT	20–100	2.00–10.00	>15	MIB <30 Hz, −15<SR<−5 Hz/s
Atl_FinWhale_21 Atl_FinWhale_21_HT	10–40	0.40–3.00	>6	f_{min} <17 Hz, 20< f_{peak} <22 Hz, −100<SR<0 Hz/s
Atl_FinWhale_21.2 Atl_FinWhale_21.2_HT	8–40	0.30–3.00	>6	f_{min} <17 Hz, −100<SR<0 Hz/s
Atl_FinWhale_130	110–150	0.30–1.50	>6	f_{min} <125 Hz
VLFMoan	10–100	0.30–10.00	>10	f_{min} <40 Hz
N_RightWhale_Up1	65–260	0.60–1.20	70–195	f_{min} <75 Hz, 30<SR<290 Hz/s
N_RightWhale_Up2	65–260	0.50–1.20	NA	30<SR<290 Hz/s
N_RightWhale_Up3	30–400	0.50–10.00	>25	10<SR<500 Hz/s
SeiWhale_LowThreshold	20–100	1.00-1.70	30-80	MIB <100 Hz, f_{peak} <50 Hz, −80<SR<−12 Hz/s
SeiWhale_MidThreshold	20–80	1.00–1.70	30–80	MIB <100 Hz, −80<SR<−12 Hz/s
SeiWhale SeiWhale_HighThreshold	20–150	0.50–1.70	19–120	MIB <70 Hz, −100<SR<−6 Hz/s

f = frequency, MIB = median instantaneous bandwidth, SR = sweep rate; HT = high threshold; BW = bandwidth

Table B-3. A sample of vocalization sorter definitions for the tonal pulse train vocalizations of cetacean species expected in the area.

Automated detector	Target species	Frequency (Hz)	Pulse duration (s)	Inter-pulse interval (s)	Train duration (s)	Train length (# pulses)
NarwhalKnockTrain	Narwhal	1000–8000	0.005–0.04	0.03–0.5	0.5–30	6–100

B.3. Automatic Data Selection for Validation (ADSV)

To standardise the file selection process for the selection of data for manual analysis, we applied our Automated Data Selection for Validation (ADSV) algorithm. Details of the ADSV algorithm are described in Kowarski et al. (2021) and a schematic of the process is provided in Figure B-5. ADSV computes the distribution of three descriptors that describe the automated detections in the full data set: the Diversity (number of automated detectors triggered per file), the Counts (number of automated detections per file for each automated detector), and the Temporal Distribution (spread of detections for each automated detector across the recording period). The algorithm removes files from the temporary data set that have the least impact on the distribution of the three descriptors in the full data set. Files are removed until a pre-determined data set size (N) is reached, at which point the temporary data set becomes the subset to be manually reviewed.

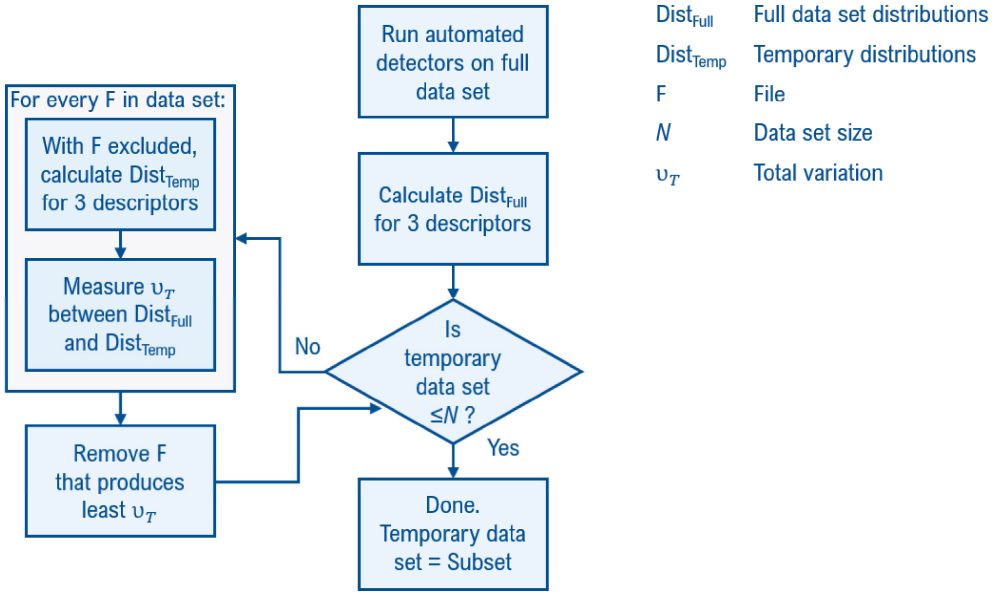

Figure B-5. Automated Data Selection for Validation (ADSV) process based on Figure 1 from Kowarski et al. (2021).

B.4. Automated Detector Performance Calculation and Optimization

All files selected for manual validation were reviewed by an experienced analyst using JASCO's PAMlab software to determine the presence or absence of every species, regardless of whether a species was automatically detected in the file. Although the automated detectors classify specific signals, we validated the presence/absence of species at the file level, not the detection level. Acoustic signals were only assigned to a species if the analyst was confident in their assessment. When unsure, analysts would consult one another, peer reviewed literature, and other experts in the field. If certainty could not be reached, the file of concern would be classified as possibly containing the species in question or containing an unknown acoustic signal. Next, the validated results were compared to the automated detector results in three phases to refine the results and ensure they accurately represent the occurrence of each species in the study area.

In phase 1, the human validated versus automated detector results were plotted as time series and critically reviewed to determine when and where automated detections should be excluded. Questionable detections that overlap with the detection period of other species were scrutinized. By restricting detections spatially and/or temporally where appropriate, we can maximize the reliability of the results.

In phase 2, the performance of the automated detectors was calculated and optimized for each species using a threshold, defined as the range of the number of automated detections per file within which detections of species were considered valid (bounded by a minimum and maximum).

To determine the performance of each automated detector and any necessary thresholds, the automated and validated results (excluding files where an analyst indicated uncertainty in species occurrence) were fed to a maximum likelihood estimation algorithm that maximizes the probability of detection and minimizes the number of false alarms using the Matthews Correlation Coefficient (MCC):

$$MCC = \frac{TPxTN - FPxFN}{\sqrt{(\mathrm{TP}+\mathrm{FP})(\mathrm{TP}+\mathrm{FN})(\mathrm{TN}+\mathrm{FP})(\mathrm{TN}+\mathrm{FN})}}$$

$$P = \frac{TP}{TP+FP}; R = \frac{TP}{TP+FN}$$

where *TP* (true positive) is the number of correctly detected files, *FP* (false positive) is the number of files that are false detections, and *FN* (false negatives) is the number of files with missed detections.

In phase 3, detections were further restricted to include only those where *P* was greater than or equal to 0.75. When *P* was less than 0.75, only validated results were used to describe the acoustic occurrence of a species. The occurrence of each species was plotted using JASCO's Ark software as time series showing presence/absence by hour over each day.

DOCUMENT CONTROL DATA

*Security markings for the title, authors, abstract and keywords must be entered when the document is sensitive

1. ORIGINATOR (Name and address of the organization preparing the document. A DRDC Centre sponsoring a contractor's report, or tasking agency, is entered in Section 8.)

JASCO Applied Sciences (Canada) Ltd
20 Mount Hope Avenue
Dartmouth, NS B2Y 4S3

2a. SECURITY MARKING (Overall security marking of the document including special supplemental markings if applicable.)

CAN UNCLASSIFIED

2b. CONTROLLED GOODS

NON-CONTROLLED GOODS
DMC A

3. TITLE (The document title and sub-title as indicated on the title page.)

Soundscape Characterization and Marine Mammal Occurrence: Western Baffin Bay, September 2022–23

4. AUTHORS (Last name, followed by initials – ranks, titles, etc., not to be used)

Delarue, J.; Wilson, C.; Richardson, A.

5. DATE OF PUBLICATION (Month and year of publication of document.)	6a. NO. OF PAGES (Total pages, including Annexes, excluding DCD, covering and verso pages.)	6b. NO. OF REFS (Total references cited.)
March 2024	61	64

7. DOCUMENT CATEGORY (e.g., Scientific Report, Contract Report, Scientific Letter.)

Contract Report

8. SPONSORING CENTRE (The name and address of the department project office or laboratory sponsoring the research and development.)

DRDC – Atlantic Research Centre
Defence Research and Development Canada
9 Grove Street
P.O. Box 1012
Dartmouth, Nova Scotia B2Y 3Z7
Canada

9a. PROJECT OR GRANT NO. (If appropriate, the applicable research and development project or grant number under which the document was written. Please specify whether project or grant.)	9b. CONTRACT NO. (If appropriate, the applicable number under which the document was written.)
DNA_028	R.127481.001

10a. DRDC PUBLICATION NUMBER (The official document number by which the document is identified by the originating activity. This number must be unique to this document.)	10b. OTHER DOCUMENT NO(s). (Any other numbers which may be assigned this document either by the originator or by the sponsor.)
DRDC-RDDC-2024-C167	PO 700748104

11a. FUTURE DISTRIBUTION WITHIN CANADA (Approval for further dissemination of the document. Security classification must also be considered.)

Public release

11b. FUTURE DISTRIBUTION OUTSIDE CANADA (Approval for further dissemination of the document. Security classification must also be considered.)

12. KEYWORDS, DESCRIPTORS or IDENTIFIERS (Use semi-colon as a delimiter.)

Marine Mammal Mitigation; Marine Mammals; Ocean Ambient Noise; Ambient Noise

13a. ABSTRACT (when available in the document, the English version of the abstract must be included here.)

JASCO Applied Sciences (JASCO) was contracted by Defense Research and Development Canada (DRDC) to assist with the analysis of long-term Passive Acoustic Monitoring (PAM) data from Baffin Bay. DRDC deployed three moorings with Autonomous Multi-channel Acoustic Recorders (AMARs) along the western side of Baffin Bay in August of 2022 and retrieved them in September 2023 (Figure 1). JASCO was tasked with downloading the three year-long AMAR recordings and performing a basic analysis of the data to identify data quality issues, if any, and to characterize ambient sound and provide a basic description of vessel and marine mammal presence. This report presents the results of these analyses and identifies topics worthy of further investigation.

13b. RÉSUMÉ (when available in the document, the French version of the abstract must be included here.)

JASCO Applied Sciences (JASCO) a été retenu par Recherche et développement pour la défense Canada (RDDC) pour aider à l'analyse des données de surveillance acoustique passive (PAM) à long terme de la baie de Baffin. RDDC déployé trois amarres avec des enregistreurs acoustiques multicanaux autonomes (AMAR) le long de la côte oust côté de la baie de Baffin en août 2022 et les ont récupérés en septembre 2023 (figure 1). JASCO a été chargé en téléchargeant les enregistrements AMAR de trois ans et en effectuant une analyse de base des données pour identifier les problèmes de qualité des données, le cas échéant, et caractériser le son ambiant et fournir une description de base de présence de navires et de mammifères marins. Ce rapport présente les résultats de ces analyses et identifie sujets qui méritent une étude plus approfondie.